THE UNIVERSITY OF QUEENSLAND

School of Information Technology and Electrical Engineering

Cooperative Control of the Dual Gantry-Tau Robot

By

Rosmawati Mat Zain
(40922171)

School of Information Technology and Electrical Engineering
The University of Queensland

MAY 2006

Declaration

The work presented in this thesis is original and has not been previously submitted under any circumstances in whole or in part at the University of Queensland or any other institution. This work was performed under the supervision of Dr. Geir Hovland.

Concepts and material established by previous authors and presented as the foundation of this thesis have been referenced in the text and footnotes.

Rosmawati Mat Zain

Acknowledgement

This thesis would not have been possible without the help and support of many other people. I would like to express sincere gratitude and thanks to the following people;

- My supervisor, Dr. Geir Hovland, for his continuous support and guidance throughout the project duration. His valuable advice and technical expertise are greatly appreciated.

- Michael Berghauser, the previous student who design and work on the Dual Gantry-Tau machine, for helping me with the familiarization of the machine and equipments used in the project. Similarly to Matthew Murray who have previously worked on the Gantry-Tau before.

- My family and friends for their great understanding and moral support.

Abstract

Utilization of multiple parallel robots operating in the same work place and cooperating on the same job have opened up new challenges in coordination control strategies. Multiple robot control is a natural progression for Parallel Kinematic Machines (PKM) as it offers many of the desirable qualities especially in cooperative arrangements where multiple robots can be associated with an easily reconfigurable parallel machine. These special characteristics allow much faster and precise manipulations especially in manufacturing industries. With the possibility of cooperative control architecture, PKMs will be able to perform many of the tasks currently requiring dual serial robots such as complex assemblies, heavy load sharing and large machining jobs.

This project aimed to develop a coordinated control strategy for the Gantry-Tau robot. The Gantry-Tau robot was successfully built last year under an undergraduate thesis at the University of Queensland. This new design accommodated dual tool points which allow both cooperative and independent task sharing. This created the possibility for broader control strategies to be address in this project.

The scope and goal of this thesis is to successfully design a coordinated control system for the two robot's manipulators. It focuses on the development of a dual tool points synchronization technique for cooperative task sharing. This involves extending the existing control system of the Gantry-Tau to accommodate coordination control. The end result of this project will be demonstrated by connecting the two robot's arms with a string, and moving the string within the workspace without allowing it to be loosened or broken.

Table of Contents

List of Figures

List of Tables

Chapter 1

1 Introduction

1.1 Topic Definition

This project focuses on coordination control strategy particularly for parallel robots. Robots with parallel mechanisms have lead to numerous research activities since they offer tremendous advantages particularly in industry as opposed to their traditional serial counterparts. Parallel robots are spatial mechanical structures that consist of closed kinematics chains [1]. In general, a parallel topology is made up of two platforms. One of them is fixed to the reference frame and the other can have random motions in space. Various benefits of these mechanisms include high rigidity, high accuracy and low moving inertia. These special characteristics allow much faster and precise manipulations.

As the use of two or more robots working cooperatively on the same job has become an increasing trend on manufacturing floors, coordination control is a central issue that needs to be addressed. The basic objective of coordinated control of multiple robots is to be able to command the robots in such a way that the robot's arms operate in a kinematically and dynamically coordinated fashion and respond to the working environment without collisions [2]. In other words, coordination refers more specifically to the case where two robots are in contact with the same object or with each other. This mechanical contact requires higher precision, stricter synchronization and a higher level of coordination.

1.2 Project Description and Goals

A new Gantry-Tau prototype design which belongs to the PKM's family was successfully built last year under an undergraduate thesis project at the University of Queensland (Figure 1). The Gantry-Tau structure is commonly referred to as a 3/2/1 configuration which describes the clustering of its arms. The new design accommodated dual tool points as its enhancement feature [3]. The adaptation of dual tool points enhances the PKM's ability to perform many of the tasks currently requiring dual serial robot arms such as complex assemblies, heavy load sharing and large machining jobs.

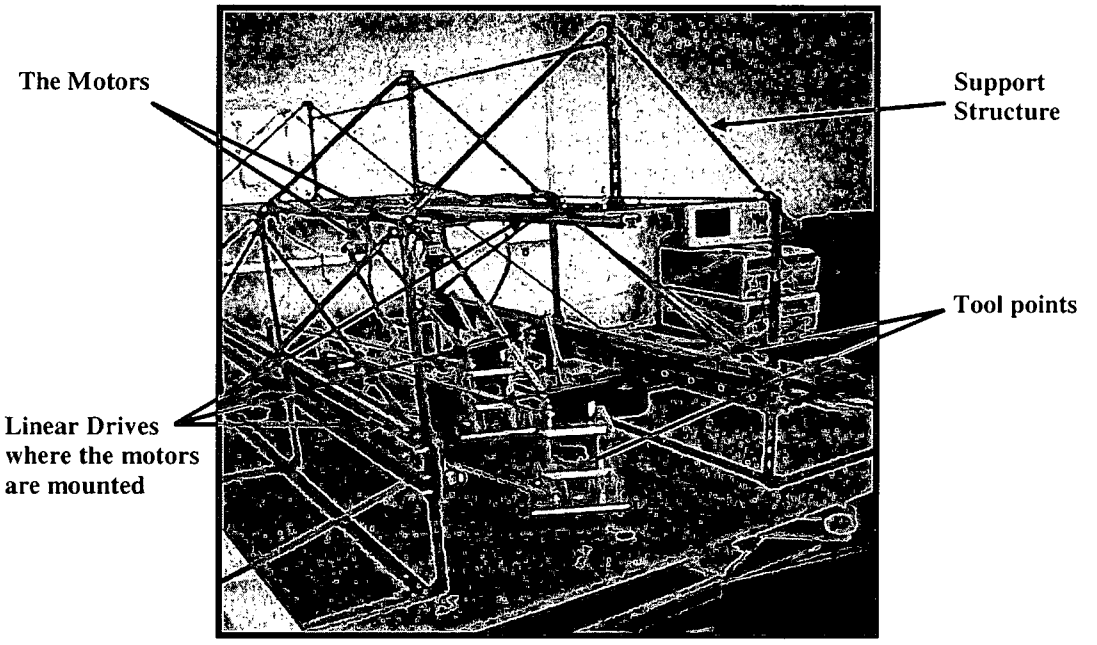

Figure 1: The Dual Gantry-Tau

Currently, the existing control system built for the Gantry-Tau only allows independent control of one of its manipulators. The control system accommodated three feedback loops to control current, velocity and position which are fed through a simple PID controller. However, the potential of the dual tool point's capability and adaptability has not been fully realised with the current control system. Thus, this project aims to expand Gantry-Tau performance through the facilitation of coordinated motion control.

The overall goal of this project is to analyse and design a coordinated control system for the two robot's manipulators. The basic aims of the coordinated control of the two manipulators are to precisely control the movement of the individual manipulator to track the desired trajectories, and to efficiently synchronize the motion of the manipulators to minimize the positional offsets between them.

The end result of this project will be demonstrated by connecting the two robot's arms with a string and to move the string within the workspace without allowing it to be loosened or broken.

1.3 Motivation

Utilization of multiple robots operating in the same work space and cooperating on the same job have opened up new applications in manufacturing industries. Interest in coordinated motion control of multiple manipulators is high due to the following potential applications;

i. Complex assembly and material handling tasks
ii. Manipulation of large and heavy objects
iii. Servicing and maintenance in hazardous environments

Apart from that, multiple coordinated manipulators could also be the solution to reduce the time required to complete an assembly task and minimize external fixture requirements. The control problem of multiple arms represents a significant increase in complexity over the single arm case and thus will be the major challenges for this project.

1.4 Chapter Outlines

The remainder of this thesis is divided into 6 sections.

Chapter 2: Literature Review

This chapter provides the details of relevant background towards further understanding of this thesis based on previous documentation. This includes in depth discussion on the types of Parallel Kinematics Machines and variations in the Gantry-Tau PKM as well as classification of coordinated control techniques.

Chapter 3: Theoretical Formulation

This chapter outlines the theoretical information particularly in the coordinated control techniques and modelling of the Gantry-Tau system. All the necessary theoretical procedures and simulation results will be presented in this chapter.

Chapter 4: Practical Implementation

This section describes the actual implementation of the software components (the control system) and the hardware (The Gantry-Tau) including all the necessary modifications and the design process.

Chapter 5: Results

This section illustrates the results that were obtained from the practical implementation.

Chapter 6: Discussions and Critical Review

This section analyses the results as well as the reasoning on which the conclusions are then founded.

Chapter 7: Conclusions

Finally, this chapter presents the conclusions that can be made from the completion of the project. Possible future improvements and research directions are also highlighted.

Chapter 2

2 Literature Review

The purpose of this chapter is to draw attention towards information relevant in understanding the development of the coordinated control scheme for the Gantry-Tau robot. In this section, the general descriptions of parallel robots as well as examples of parallel robots are first briefly surveyed. The architecture, advantages and disadvantages of these types of parallel robots will be investigated and compared with the Gantry-Tau structure. Secondly, the coordinated control approaches that are currently available will be examined and considerations that were made in choosing the most suitable scheme for the Gantry-Tau will be explained.

2.1 Background Information

2.1.1 Parallel Kinematics Machine (PKM)

Parallel robots possess characteristics that are particularly suited to a number of typical manufacturing applications such as packaging and assembly. As a result, several new structures and mechanisms have been developed and enhanced to suit increasing demand. A parallel robot is "a closed-loop mechanism of which the end-effector is connected to the base by a multiple of independent kinematic chains" **[4]**.

In general, parallel robots are often classified by the number and type of degree of freedom (DoFs) they posses. However, they share a common closed-loop mechanism which offers them good performance in terms of accuracy, rigidity and ability to manipulate large loads **[4]**. The following figure shows an example of PKM with Delta configuration, the IRB 340 Flexpicker from ABB.

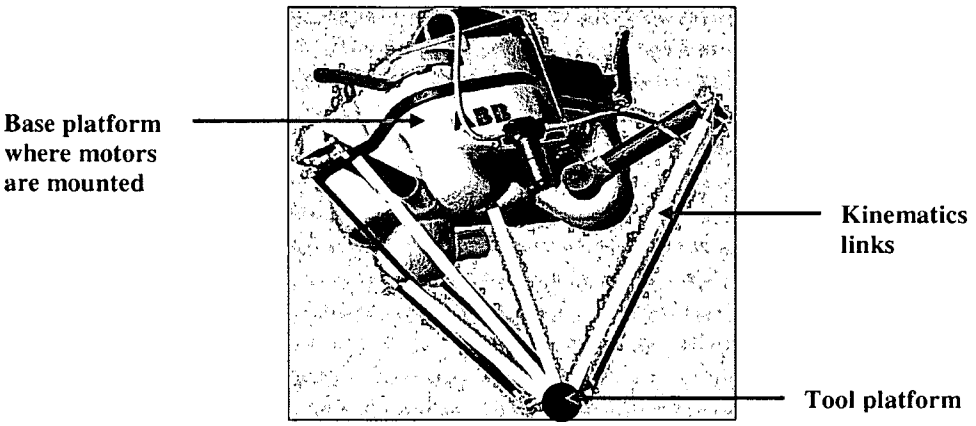

Figure 2: Closed Kinematics Chains of Parallel Robot

As can be seen from Figure 2, all actuated links represented in yellow are kinematically parallel and eventually meet at the end-effector where the tool point is located. The advantages of having this topology are well known as:

i. The position error of the end-effector is an average error in each link instead of cumulative errors in serial structures
ii. It reduces the overall weight of the structure since electrical motors are not supported by the link but are mounted on the base platform
iii. It increases the stiffness and speed of the system
iv. More accurate and faster manipulations than the current serial mechanism
v. Simpler inverse kinematics but more difficult forward kinematics

These competitive features of PKM are well suited to various applications in manufacturing industries particularly pick and place, assembly, laser cutting, drilling, milling and many more. However, many of the PKM structures are also known for their limitations of having smaller workspaces "that can be seen as the intersection of the individual workspace of each serial arm constitute the robot" [5]. Therefore, the Gantry-Tau topology has designed to overcome this limitation while retaining most of the PKM's advantages.

The following sub-sections provide several examples of PKMs that are currently dominating the manufacturing floors. The Gantry-Tau structure and variations in its configuration are presented in section 2.1.2.

2.1.1.1 DELTA Robot [6]

The DELTA robot was invented in 1986 by R. Clavel and his co-workers at the Swiss Federal Institute of Technology, Lausanne. It is known as the most successful parallel robot design and the fastest robot of its kind. As seen from Figure 2 and 3, the tool base platform is linked to the robot base (located at the top) by three identical closed kinematic chains consisting of arms and parallel rods which are actuated by three revolute electric motors. These result in three translatory degrees of freedom for the robot tool-base. A constant orientation of the platform is maintained since each parallelogram joint prevents the rotation movement around one axis thus making the structure very rigid.

The possibility of keeping the motors fixed on the base allows a large reduction of the active mobile mass of the robot structure. Thus the topology is well suited to fast execution of light duty tasks.

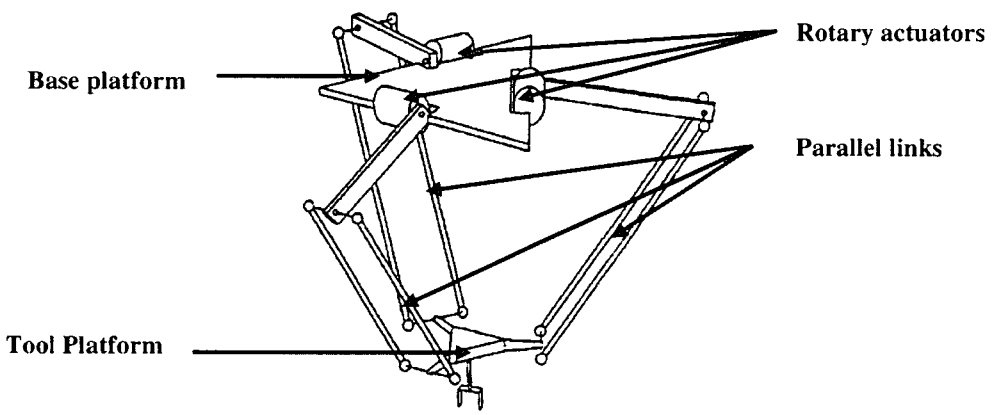

Figure 3: The DELTA Robot [7]

2.1.1.2 H4 Robot **[8]**

H4 originated in France and joined the family of parallel robot due to fact that 3 DoFs are not enough for most pick and place applications. Thus the proposed H4 structure by Pierrot and Company provided 4 DoFs (3 translations to move the carried object from one point to the other, 1 rotation to arrange the object in its final location). As its name suggests, the mechanism is based on 4 independent kinematic chains between the base and the tool platform known as the nacelle. As with the DELTA, each chain is actuated either by a linear or rotary actuator and each actuator is fixed on the base. The design of H4, either symmetrical or asymmetrical, shows an effective solution to most industrial applications. Figures 4(a) and 4(b) illustrate the common topology of the H4 structure.

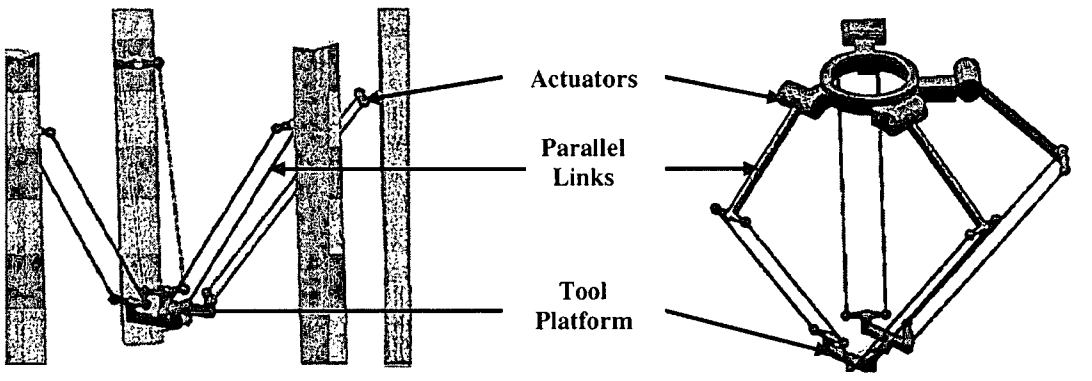

Figure 4(a): The H4 Robot with symmetrical design [9]

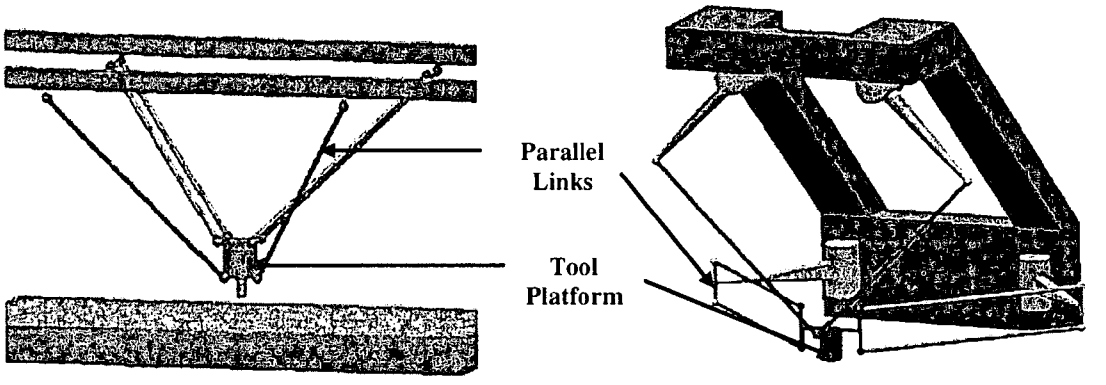

Figure 4(b): The H4 robot with asymmetrical design [9]

2.1.1.3 Triglide Robot **[10]**

The design synthesis and modelling of the triglide robot was achieved by Hervé and Sparacino in France in 1991. The triglide structure, better known as the star topology is made up of three identical cooperating arms. These manipulator arms converge to a common point where the mobile platform is located. As a result, three translatory motions are realized and an additional rotational axis is mounted on the working platform to enable the orientation of the gripper. The configuration is similar to DELTA except that the actuator is driven by three linear direct drives instead of revolute drives. The triglide structure is depicted in Figure 5 below.

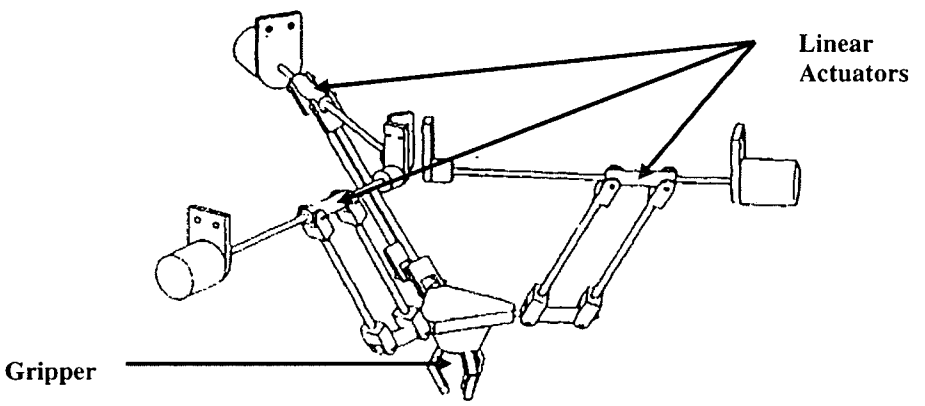

Figure 5: The Triglide Robot [10]

2.1.2 The Gantry-Tau

The Tau family of parallel kinematic manipulators was introduced by ABB Robotics **[11]** in Sweden. Gantry refers to the actuated linear links arrangement. The Tau structure refers to the links that are clustered as 3/2/1, 3/1/2, 2/3/1, 2/1/3, 1/3/2 or 1/2/3 thus making it a six links parallel kinematics structure. This allows the structure to be constrained to 3 DoFs and form a closed kinematic chains. A typical structure of the Gantry-Tau is shown in the Figure 6.

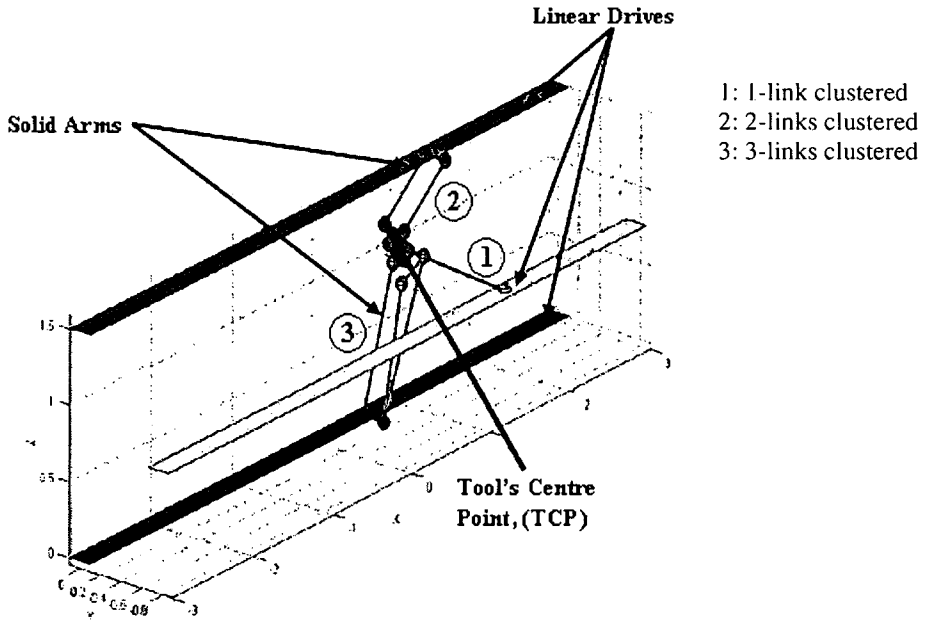

Figure 6: The Gantry-Tau Structure [12]

As stated before, the benefit of the Gantry-Tau structure is that it overcomes the main drawback of the small workspaces of most parallel structures. The Gantry-Tau structure has already demonstrated its capabilities with respect to existing industrial applications. Some variations of this structure can be seen and they are described in the next sub-sections.

2.1.2.1 Tau with all links in the 3-arm cluster parallel.

The first constructed Gantry-Tau (Figure 7) with the 3-links clustered in parallel, is by Johannesson **[13]**. The 3/2/1 clustering approach is designed to constrain all 6 degrees of freedom without redundancy. Workspace optimization can be easily achieved by extending the linear drives to create extra workspace as needed.

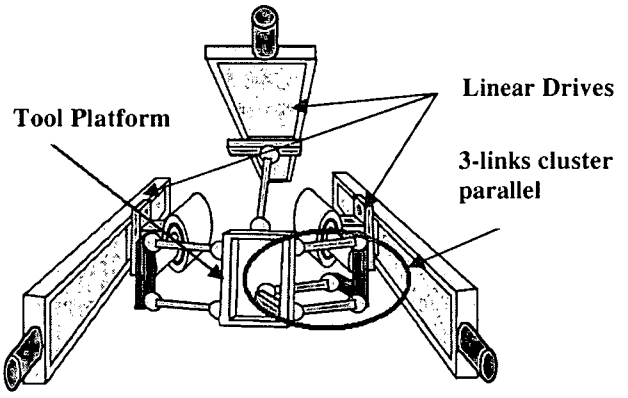

Figure 7(a): Tau 3-links cluster parallel [13]

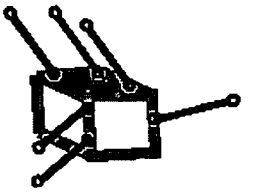

Figure 7(b): 3/2/1 Clustering

2.1.2.2 Triangular version of the Tau

The first triangular link-pair design of the Gantry-Tau was constructed at The University of Queensland in 2004. Apart form having the benefit of a large workspace, the design optimization of the triangular structure is the ability to change the configuration at both ends of the workspace.

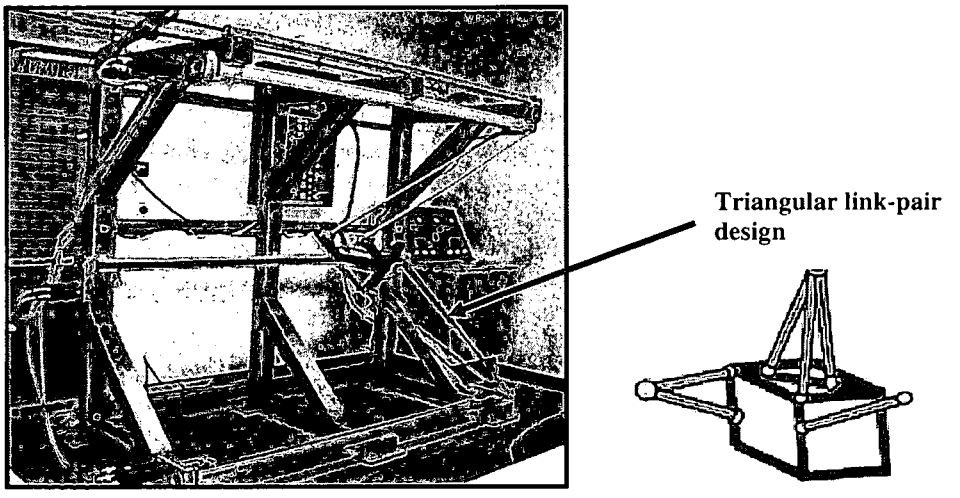

Figure 8: Triangular version of Tau [12]

2.1.2.3 The SCARA Tau

Another variation of the Gantry-Tau is the SCARA Tau presented by Brogardh **[11]**, using 3/2/1 clustering. This structure uses a rotary drive instead of a linear drive which gives the motion pattern as for a Scara robot. As can be seen from Figure 9, the whole robot structure can be rotated around the fixed platform, giving a large workspace for the robot.

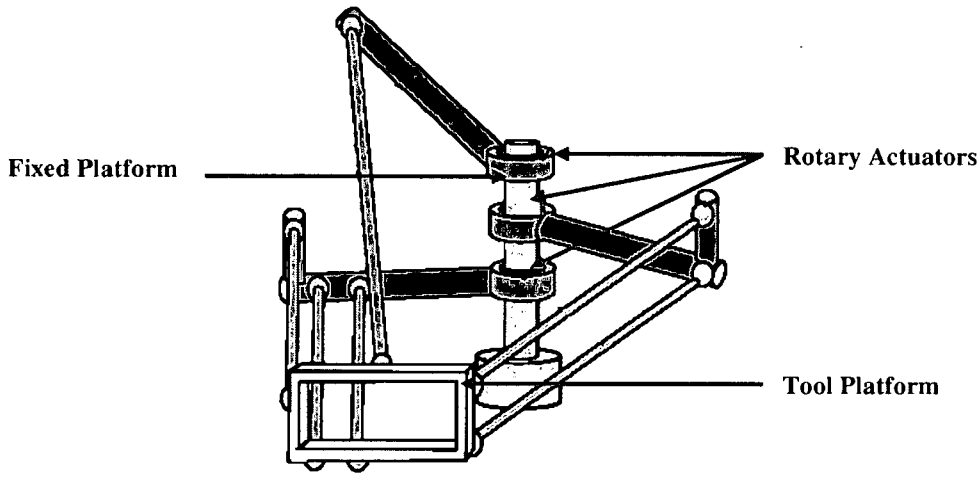

Figure 9: The SCARA Tau [11]

2.1.2.4 Gantry-Tau with dual tool point

Further optimization of the Gantry-Tau design was achieved through the development of the Dual Gantry-Tau constructed in 2005 at The University of Queensland (Figure 1). This new design had adapted the previous triangular link-pair design to accommodate dual tool points. The configuraton allows both cooperative and independent task sharing.

2.1.3 Comparison of PKMs

There are some similarities between the triglide and H4 to the Gantry-Tau structure **[13]**. The similarities are based on the number of DoFs that the structures provide and they both utilize linear drive actuators. The Triglide structure, which is sometimes called the linear Delta, suffer from a small workspace compared to its foot print. As with the Delta, its configuration is not optimal in terms of workspace volume and suffers from a lack of stiffness at the workspace boundary. Meanwhile, the H4 architecture with 2/2/2/2 arrangement of its 8 arms may be redundant. This is because, most of the robotized tasks do not need all 6 DoFs and thus only 6 arms are needed for such tasks.

Apart from that, the Delta configuration is also very similar to the Tau but with 2/2/2 configuration and it is of revolute motor drives instead of linear drive. The 3/2/1 configuration of the Tau may be better if the robot needs to support a large force in a particular direction. It had been reported that the Tau has the highest stiffness in the Z-direction. Thus the 3-arm cluster in Tau configuration can support the force effectively in that direction. As with the triangular version of the Gantry-Tau, the significant advantage can be visualized through the possibility of reconfiguration. With the parallel 3-arm cluster, the robot might only be efficient in one end of the workspace. On the other hand, the triangular Tau can provide better solutions at both ends of the workspace.

The following table gives a comparative study of the PKMs mentioned in this paper. Particular attention is given to compare the advantages and disadvantages associated with each architecture.

	Gantry-Tau	DELTA	H4	Triglide
Degree of Freedom	3 translational	3 translational	3 translational + 1 rotation about a given axis	3 translational + 1 rotation mounted on workspace
Applications	Water-jet cutting, laser-cutting of sheet metal, milling of patterns, cutting and edges cleaning of glass, wood, plastics etc	High-speed application of light duty task. Eg: pick and place	High speed handling in robotics and milling in mechanical tool industry	Pick and place jobs such as sorting, arranging on palettes, packaging and assembly
Advantages	• Greater stiffness, increase load capacity and better utilization of workspace • The triangular version enables reconfiguration of the robot **[13]** • The 3/2/1 arrangement provides more support of a large force in particular direction	• Higher rigidity, speed and precision	• Wide workspace as well as high speed **[16]**	• Possesses the greatest percentages of its workspace having a good dexterity **[15]**
Disadvantages	–	• Lack of stiffness at workspace extremities **[17]** • Short service life **[17]** • Its configuration is not optimal in term of workspace volume **[18]** • Limited application since DoFs are too small to perform a complicated tasks **[16]**	• Bad arrangement of actuators leading to singularity configurations, non-homogenous behaviour in work space and bad stiffness **[17]** • Redundant arms leading to complex assembly of this robot	• Small workspace

Table 1: Comparison of PKMs

2.2 Coordinated Control of Multiple Robot Manipulators

2.2.1 Type of Coordinated control

As mechanical design and modeling of PKMs are the key factors for effective performance, so is the control system. This particularly true in the current manufacturing situation where the use of more than one robot in a workspace has increased and the ability to coordinately control the robots is vital. A multiple robot task enables the following conditions **[19]**;

i. The robots are kinematically constrained, i.e., all robots grasp a common rigid payload and they are physically connected
ii. The robots are not physically connected, but perform a common task

Thus application of coordinated control can be classified into the following types;

Type 1: *Each robot performs its own task independently in a shared common workspace*

Example: *One robot manipulates a rigid payload while the other spread adhesive on the edges with both robots in motion simultaneously*

Type 2: *All robots cooperate to perform a common given task*

Example: *Two robots carrying a load cooperatively in an assembly line*

The control of type 1 system presents the advantage of doubling productivity and workspace. However, the control challenge of this type is to avoid collision between the robots and to ensure accurate path planning. On the other hand, the type 2 system presents a much broader problem as care must be taken to ensure that constraints for relative position and force are well controlled. Even so, significant gains in load capacity and relative stiffness of the system can be achieved through this type of control.

2.2.2 *Method for Coordinated Control*

As reported in the literature, coordination schemes are categorized under one of the following three types; (1) the master/slave control; or (2) the centralized control; or (3) the decentralized control **[19]**. In these coordination techniques multiple manipulators are considered to be physically connected together for assembly tasks (i.e grasping a payload). All the possible coordination techniques will be reviewed in terms of their pros and cons in order to select the most appropriate approach to suit the Gantry-Tau robot.

2.2.2.1 *The master/slave control* **[20]**

The most commonly used technique is the classical master/slave arrangement where two robots play different roles. In this approach, one robot is assigned as the master and the other as the slave. The master is designed to track the planned path under position control and the slave is controlled to follow the master's trajectories via a kinematic constraint relationship **[21]** in order to achieve synchronization in motion. Figure 10 briefly shows a block diagram of the master/slave control scheme.

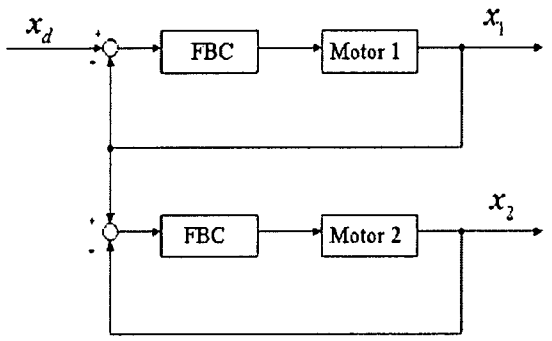

Figure 10: Block diagram of the master/slave control scheme [20]

This technique is fairly simple but it requires fast processing and high feedback gains to ensure smooth coordination between the robots. For a more robust variation of this scheme, the hybrid/force feedback technique may be implemented which allows the movement of the slave in relation to both position and relative force of the master. However, this is rather complicated and requires greater effort at the control level since the position and force at any given time must be known.

The master/slave scheme is an effective method to use during jogging and homing moves. However, the architecture is known to have the drawback of communication delay and lack of coordination between the robot arms **[22]**. Furthermore, for a system with similar resonant frequency, inaccuracy can build up due to the fact that any deviation in the master robot will be fed into the slave and get amplified significantly. On top of that, there is no clear way that the master robot will be able to know when the slave motor encounters a disturbance and to response to such problems.

2.2.2.2 The centralized control **[21], [23], [24]**

The second scheme is of a centralized control architecture where a single controller is supposed to control all the manipulators. In this technique, the robots and the grasped payload are considered as a closed kinematic chain. This method is designed based on a unified robot and payload dynamic model. Figure 11 depicts an example of the centralized coordinated control architecture.

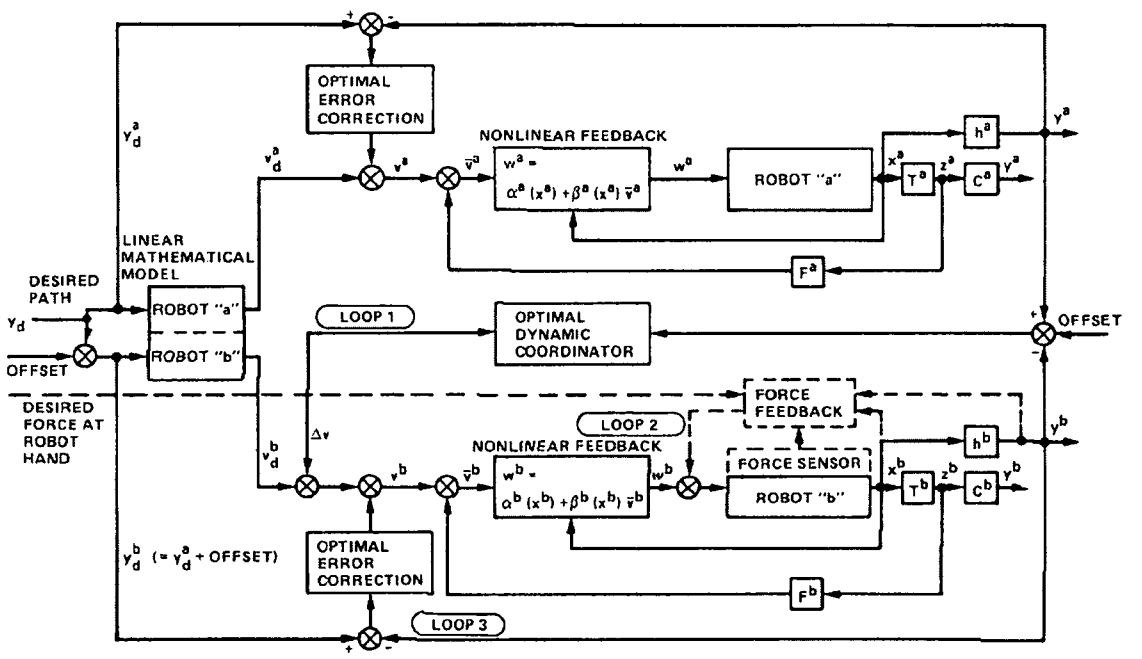

Figure 11: Centralized coordinated control architecture [24]

There are two crucial design steps for this architecture as seen in the block diagram above. The first step is the linearization of the manipulator dynamics by nonlinear feedback. The second step is the design of position and force controllers for the linearized model. The control strategy proposed by Tan, Bejczy and Yun **[24]** is to use a dynamic coordinator acting on relative position and velocity errors and/or on relative force-torque errors between the two arms.

The merit of this scheme lies on the robustness of its controller to model errors **[23]** and the capability of directly responding to changing task commands **[24]**. However, the structure and dynamics approach used in the centralized coordination schemes might be complicated in terms of dealing with tasks involving multiple manipulators.

2.2.2.3 The decentralized control

The third approach is the decentralized controller in which each robot is controlled separately by its own local controller. The decentralized approach overcomes the computational burden imposed on the central controller. Figure12 provides a block diagram of the decentralized control scheme.

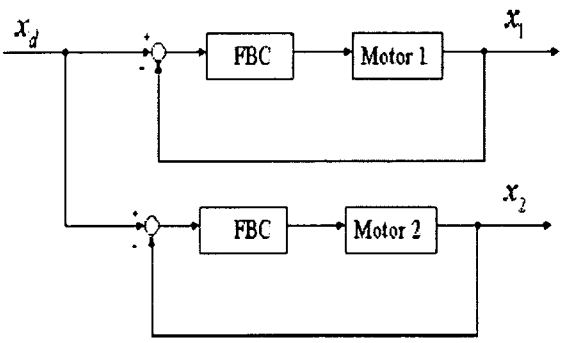

Figure 12: Block diagram of decentralized coordinated control scheme [20]

Identical desired trajectories are used as a command signal to both robots. Each feedback loop of the robots has the responsibility to track the desired path. As the deficiencies of one robot do not directly affect the other robot, this method is better compared to a master/slave mode presuming that all robots have tight feedback loops and close dynamics characteristics.

Liu, Arimoto and Ogasawara **[25]** have proposed two decentralized control algorithms for trajectory tracking of two manipulators working cooperatively in which no communication is required between the manipulators. In their design, position of each robot is controlled separately by feedback loop. The first controller uses a feedforward of the desired force to control the internal force between the object while the second controller uses a force feedback. Although the implementation of this scheme is easy, the current design of the Gantry-Tau does not allow force feedback.

Sun and Mills **[19]** have proposed a new coordination technique through an adaptive synchronized control which is of decentralized architecture. The coordination strategy is to let each manipulator track its desired trajectory while synchronizing its motion with the other manipulator's motion by feeding back the position error of each manipulator and the differential position error between two manipulators. The basic objective of this technique is to make the errors converge to zero. The controller is designed by incorporating cross-coupling technology into an adaptive-control architecture through feedback of position and synchronization errors. This approach is more straightforward without the need to explicitly employ hybrid position and force control in the controller design.

2.2.3 *Consideration for Implementation to Gantry-Tau*

The Dual Gantry-Tau in its current design is well suited to both type 1 and type 2 controls as each manipulator can operate independently at both ends of the tracks or in a cooperative mode. However, the scope of the project is limited to developing the control technique for type 2 only. The focus is to demonstrate the ability of the system to perform dual robot operations for task sharing purposes. As the current design of the Gantry-Tau does not allow for force feedback, the control design will be concentrated on constraining the relative position between the manipulators with only position control.

In order to choose the appropriate coordinated control system approach for the Gantry-Tau, a comparative study of benefits and threats imposed by the control approaches above may be helpful in determining the best solution for the Gantry-Tau. In general, the benefits and advantages of the coordinated control systems are tabulated below:

	Master/Slave	**Centralized**	**Decentralized**
Advantages	1. Simple architecture 2. Effective to use during jogging and homing	1. Robustness in control architecture and errors modelling 2. Capable of directly responding to changing task command	1. Simple arrangement and more straightforward 2. Stability of position and synchronization errors are guaranteed 3. Able to address model uncertainties and external force disturbances 4. Provides advantage of maintaining certain kinematic relationships without explicitly employing internal force controls
Disadvantages	1. Communication delays 2. No feedback of inter-robot motion offset 3. Lack of coordination between master and slave 4. Built up errors in slave robot	1. Complicated hybrid position/force controls structure 2. Requires complex dynamics modelling of the system 3. Computational burden caused by its complicated modelling	

Table 2: Comparison of the coordinated control systems

Many choices of control techniques are available and they offer significant benefits while presenting some disadvantages. This review has defined the control problems that will be faced in a broader sense and provide an insight into this project.

However, the effectiveness of the coordinated control rarely depends on the control system alone. Particularly for the Gantry-Tau system, the master/slave arrangement may be fundamentally flawed since truly coordinated control has not been realized. Meanwhile, the centralized approach suffers from complex architecture although it offers a sophisticated control solution. Thus, the decentralized adaptive synchronized control approach looks the most promising.

This approach is chosen based upon its effectiveness, more straightforward process and suitability for the gantry-Tau structure. As the deficiencies of one robot do not directly affect the other robot, the decentralized control technique is better compared to a master/slave mode presuming that all robots have tight feedback loops and close dynamics characteristics.

Chapter 3

3 Theoretical Formulations

3.1 Control System Design Based on Decentralized Architecture

Coordination of the two robot's manipulators will be done through the decentralised approach where each manipulator is controlled separately by its own local controller.

The coordination strategy is to let each manipulator track its desired trajectory while synchronizing its motion with the other manipulator's motion. This will be achieved by feeding back the position error of each manipulator and the differential position error between two manipulators. The basic objective of the technique is to make the position errors and the differential position error converge to zero.

Concisely, the proposed block diagram for the decentralized control structure can be pictured as below:

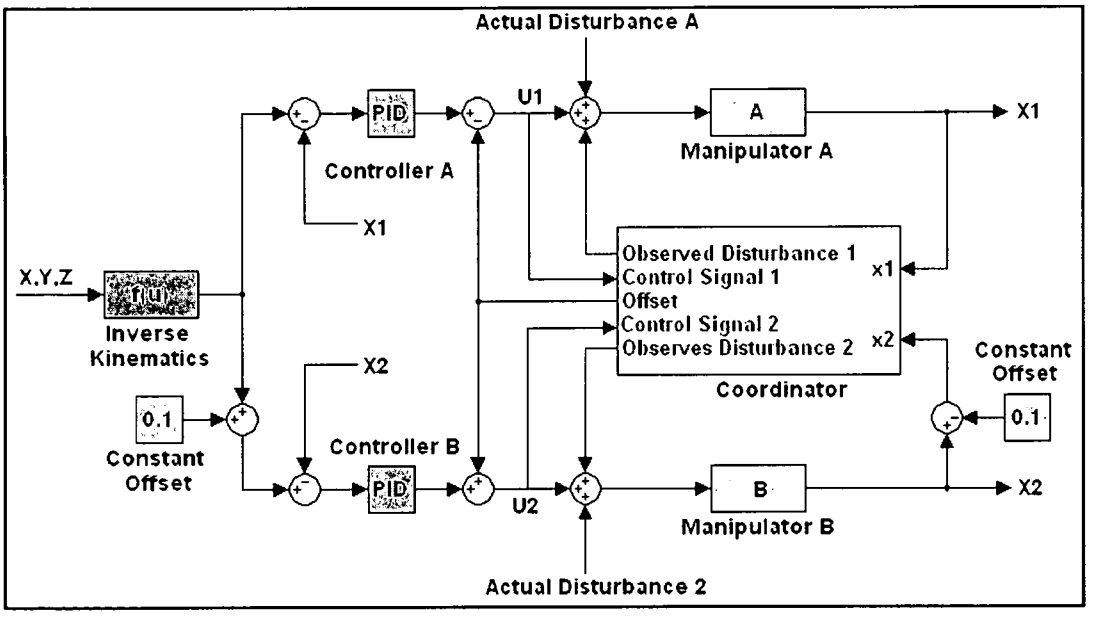

Figure 13: Overall Coordinated Control system architecture (redrawn and edited from [20])

For clarification, the purpose of each component in the control system architecture is elaborated as follows:

a) Inverse Kinematics

The inverse kinematics give the transformation from the robot arms in Cartesian coordinate (X,Y,Z) to the linear actuator position q. The inverse kinematics have already been established for the Gantry-Tau structure and can be found in **[14]**.

b) Constant Positional Offset

Identical desired trajectories are used as a command signal to both robots. Since the actuators for each manipulator are mounted on the same linear drive, a constant offset set must be introduced to set the manipulators at a constant distance apart. The constant offset can also be referred to the length of the string.

c) Individual PID Feedback Control

Each manipulator has it own controller where each feedback loop of the robots has the responsibility to track the desired path by feeding back the position error. The Technique and technical details of individual controller are presented in sub-section 3.2.

d) Coordinator and Disturbance Observer

The role of coordinator is to synchronize the motion of both manipulators by feeding back the differential position error between two manipulators. The disturbance control is also incorporated in the coordinator to compensate for disturbances arising externally in order to achieve precision movement of the gantry. Further details are discussed in section 3.3.

3.2 Typical robot control system for individual manipulator

In individual manipulator control system, PID is used as the feedback control term. This is due to effectiveness and reliability of this simple controller in most situations when adequately tuned. In this design, frequency analysis technique based on Bode plots is applied to tune PID control gains. Figure 14 shows the control technique for each individual manipulator.

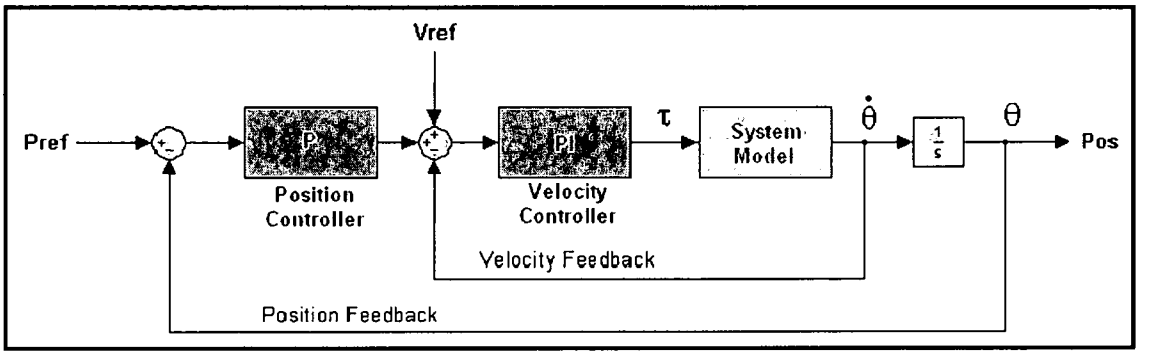

Figure 14: Robot control system

Position and velocity references are generated as input signals to the system and actual position of the manipulator is measured as an output. The control system comprises of a position controller with proportional gain, Kp and PI velocity controller. The velocity controller model comprise of a gain of the proportional function, Kp and the gain of the integrator, Ki which is in series with an intergrator, 1/s. Overall, the control system is equivalent to PID controller when view from the position output perspective.

3.2.1 Estimation of the Robot System Model

The first important step in formulating the controller's gains is to derive the system model or to estimate the transfer function representing the system. The dynamics of the system is approximated by a model consisting of a two masses connected via a gear ratio (Figure 15). The effects of spring, damper, Coulomb friction, backlash and hysteresis between the motor and the saddle **[26]** are neglected for simplification purpose. This is a significant approximation of the model and thus, it will introduce inaccuracy in modelling the system.

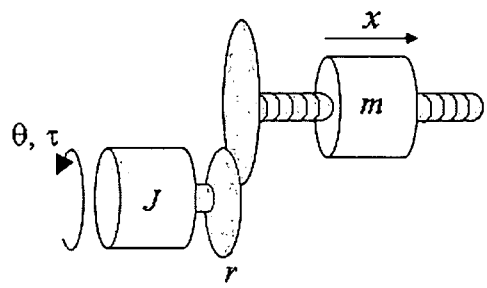

Figure 15: System Model (Redrawn and edited from [26])

The input to the system is the motor torque, τ and the output is the linear drive displacement, θ. Thus,

$$\begin{aligned}\tau &= J.\ddot{\theta} + m.\ddot{x}.r + d.\dot{\theta} \\ &= (J + mr^2)\ddot{\theta} + d\dot{\theta}\end{aligned} \qquad (1)$$

Where the physical parameters of the model are defined as:

J	moment of inertia [Nms^2]
m	mass of saddle [kg]
d	viscous friction parameter [Nm/s]
r	gear ratio [m/rad]

Rearranging equation (1) in Laplace transform yields:

$$\frac{\dot{\theta}}{\tau} = \frac{1}{(J + mr^2)s + d} \qquad (2)$$

or

$$\frac{\theta}{\tau} = \frac{1}{(J + mr^2)s^2 + ds} \qquad (3)$$

Therefore the system transfer function is estimated as a second order system having the transfer function as below:

$$\tau \longrightarrow \boxed{\frac{1}{as^2 + ds}} \longrightarrow \theta$$

where $a = J + mr^2$

3.2.2 Conceptual Idea Used to Find the System Parameters

The conceptual idea used to find the value of $J + mr^2$ and d is described below:

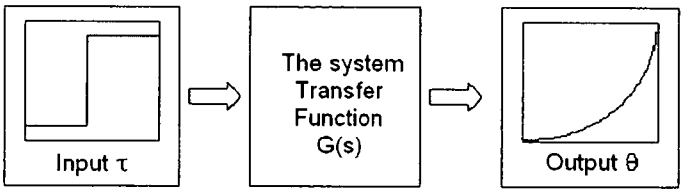

Figure 16: Conceptual Idea of Finding the System Model

From equation (1), $J + mr^2$ can be estimated by the ratio of the motor torque, τ to acceleration, $\ddot{\theta}$ for small velocity range. However, the only measured output of the system is the linear drive displacement,θ. Thus an estimation of acceleration needs to be made from the displacement response from the known displacement to acceleration relationship as below:

$$\theta = \frac{1}{2} at^2 \qquad (4)$$

The value of d can be estimated by forcing zero acceleration to the system and making the first term in equation (1) to disappear. Thus, d can be calculated by the ratio of the motor torque to velocity. An example of velocity output when torque = 0.01 is applied to the system is shown below:

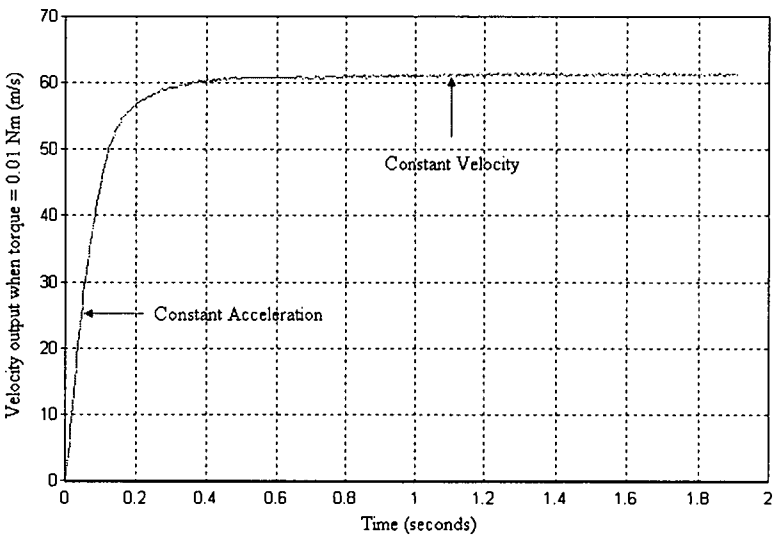

Figure 17: Velocity Output (τ = 0.01)

Several experiments have been done for several different input torques. The estimated values of $J + mr^2$ and d are tabulated below:

	Torque, τ ($\times 10^{-3}$ Nm)	Estimated Velocity (ms^{-1})	Estimated Acceleration ($\times 10^2$ ms^{-2})	d ($\times 10^{-4}$)	$J + mr^2$ ($\times 10^{-5}$)
1	1	7.586	2.190	1.32	0.457
2	2	14.483	2.928	1.38	0.683
3	3	21.379	2.690	1.40	1.115
4	4	27.586	3.332	1.45	1.200
5	5	34.483	4.148	1.45	1.205
6	6	40.000	4.550	1.50	1.319
7	7	46.552	5.804	1.50	1.206
8	8	52.083	6.373	1.54	1.255
9	9	57.500	7.311	1.57	1.231
10	10	60.476	8.206	1.65	1.219

Table 3: Estimation of System Parameter

From the data, it can be seen that for small input torque range, the system response is more dominated by the d (viscous friction) term. Meanwhile, for a bigger input torque range, the system is likely to be dominated by the $J + mr^2$ (mass) term.

It is also observed that, the estimation values are more stabilized when a bigger input torque is applied to the system. Thus, the following values will be used to represent the system model throughout the rest of the thesis.

$$G(s) = \frac{1}{1.25 \times 10^{-5} s^2 + 1.5 \times 10^{-4} s} \qquad (5)$$

3.2.3 Design of Velocity Controller (Inner loop)

Proportional Integral (PI) controller is required to be designed for the velocity controller. The basic form of the PI controller is:

$$G_C(s) = K_p + Ki/s \qquad (6)$$

The controller model comprises of a gain of the proportional function, K_P and the gain of the integrator, K_i. The proportional gain enables the rise time and system response to be adjusted and the integral gain reduces the steady state error and overshoot.

The design of these controller gains using frequency analysis technique is outline below;

Step 1a: Design Criteria

The design criteria of a controller are normally based on parameters associated with second order under-damped system response. Referring to the Figure 16, the parameters are defined as follows;

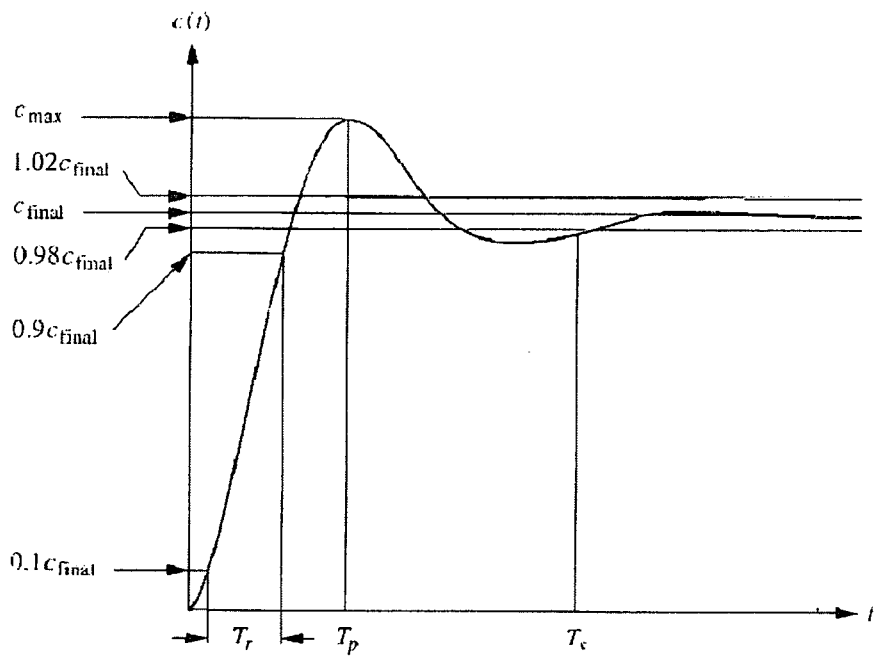

Figure 18: Second Order Under-damped Response Specification [27]

- Peak time, T_P: The time required to reach the first or maximum peak. [27]
- Percent overshoot, % OS: The amount that the waveform overshoots the steady state value at the peak time, expressed as a percentage of the steady state value. [27]
- Settling time, Ts: The time required for the transient's damped oscillation to reach and stay ±2% of the steady state value. [27]
- Rise time, T_r,: The time require for the waveform to go from 0.1 of the final value to 0.9 of the final value. [27]

For frequency analysis technique, the following design criteria are required:

T_p : 0.01 second or less

% OS : 10 % step-response overshoot

Based on these criteria, damping factor, ζ, natural frequency, ω_n and phase margin, Φ_M are calculated as below;

$$\zeta = \frac{-\ln\left(\frac{\%}{100}\right)}{\sqrt{\pi^2 + \ln^2\left(\frac{\%}{100}\right)}} = \frac{-\ln(0.1)}{\sqrt{\pi^2 + \ln^2(0.1)}} = 0.5912 \tag{7}$$

$$w_n = \frac{\pi}{T_p\sqrt{1-\zeta^2}} = \frac{\pi}{0.01\sqrt{1 - 0.3495}} = 389.52 \text{ rad/sec} \tag{8}$$

$$\Phi_M = a\tan\left(\frac{2\zeta}{\sqrt{-2\zeta^2 + \sqrt{1+4\zeta^4}}}\right) = a\tan\left(\frac{1.1823}{0.7219}\right) = 58.6^{\circ} \tag{9}$$

Step 1b: Desired Open-loop Frequency Response

The desired open-loop response is:

$$G(s) = \frac{\omega_n^2}{s^2 + 2\zeta\omega_n s} = \frac{151727.43}{s^2 + 460s} \tag{10}$$

Plotting the Bode plot for this transfer function yields:

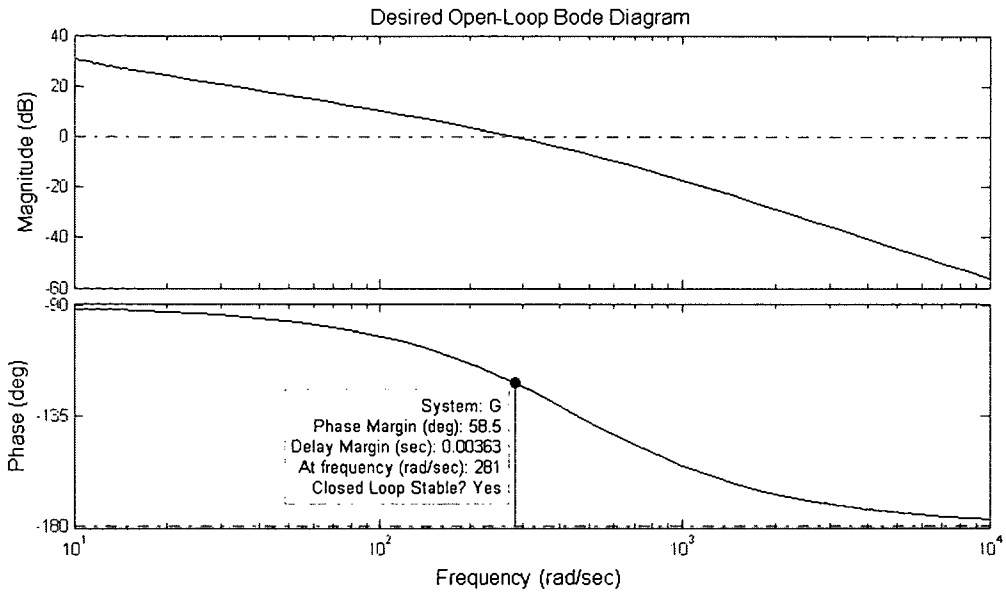

Figure 19: Desired Open-Loop Response for Inner Loop

From the plot,

Desired phase margin = 58.6 deg

At frequency, $\omega_C = 281$ rad/sec

Step 2a: Actual response with Kp = 1 and Ki = 0

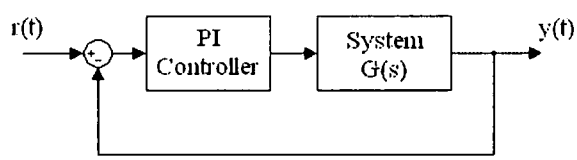

For feedback control system as above, the system transfer function equals:

$$G(s) = \frac{1}{1.25 \times 10^{-5} s^2 + 1.5 \times 10^{-4} s + 1} \qquad (11)$$

The PI controller transfer function equals:

$$G_c(s) = K_p + \frac{K_i}{s} \qquad (12)$$

Plotting the closed-loop system transfer function with Kp = 1 and Ki = 0 yields:

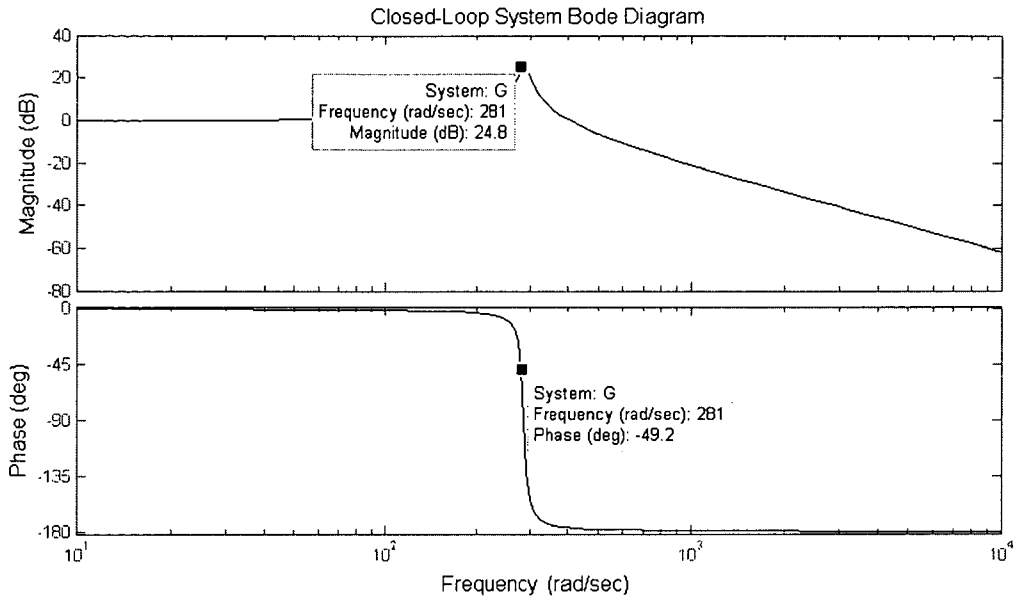

Figure 20: Closed-Loop Actual System Response (Kp = 1 and Ki = 0)

From the magnitude response:

The gain must be decreased by 24.8 dB to get ω_C at 281 rad/sec.

Converting 24.8 dB to gain yield:

$$24.8 \text{ dB} = 10^{(24.8/20)}$$

$$= 17.38$$

Thus, to decrease the gain, Kp $= 1 / 17.38 = 0.0575$

From the phase curve:

Phase margin is 130.8 deg and need to be decreased by approximately 72 deg to get the desired phase margin of 58.6 deg.

Ki/Kp is the location of zero.

Choose Ki = Kp * 281 = 16.1575 which gives a zero at 281 rad/sec.

Apart from that, a PI controller also introduces a pole at the origin which increases the order of the system by one.

Step 2b: Actual Response with Kp = 0.0575 and Ki = 16.1575

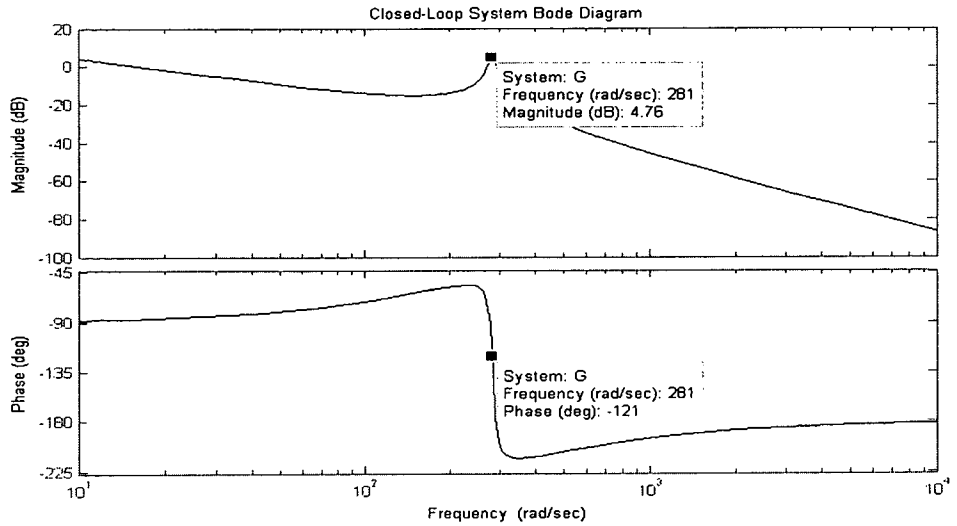

Figure 21: Closed-Loop Actual System Response (Kp = 0.0575 and Ki = 16.1575)

From the plot:

Phase margin is now correct.

But the gain has increased by 4.76 dB.

Thus fine tuning is needed by simply reduce the gain while keeping the zero.

Kp = 0.035 and Ki = 0.035 * 281 = 9.835 gives the desired result.

Step 2c: Actual Response with Kp = 0.035 and Ki = 9.835

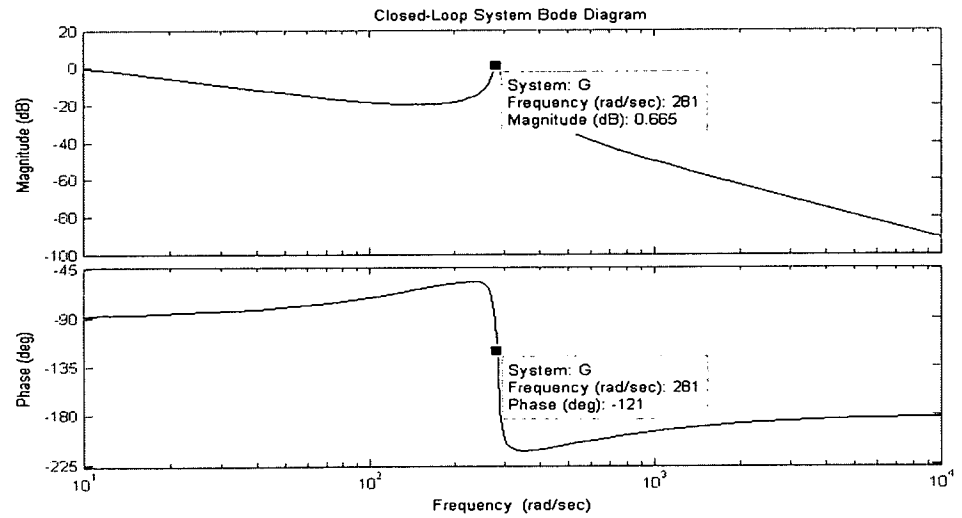

Figure 22: Closed-Loop Actual System Response (Kp = 0.035 and Ki = 9.835)

Final result from this controller design is Kd = 0.035 and Ki = 9.385. From the plot, it can be seen that the crossover frequency is 281 rad/sec and the phase margin is 60 deg which are as desired.

Step 3: Verification

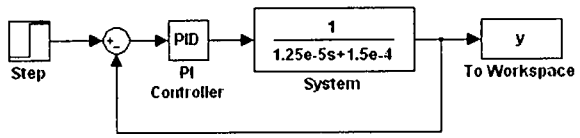

Figure 23: Simulink Verification for Inner Loop

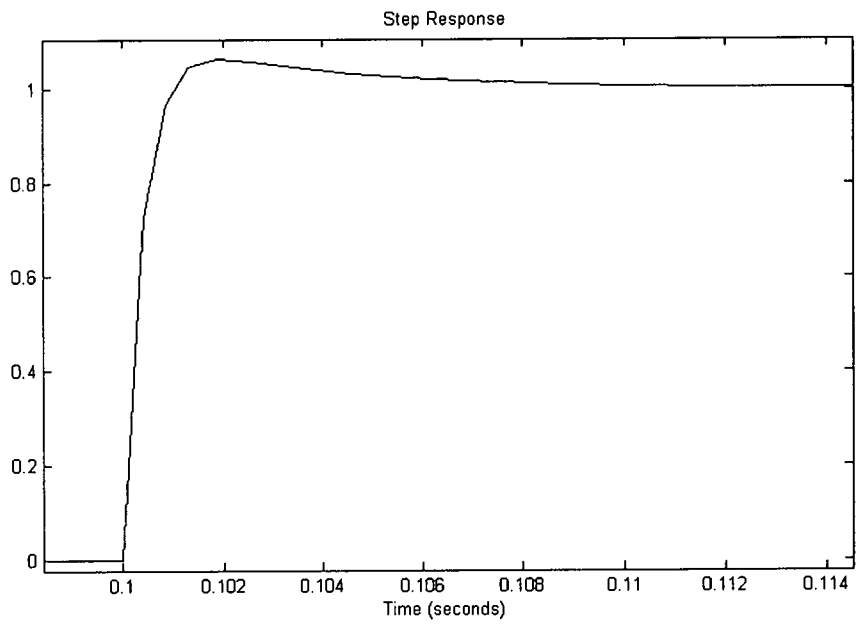

Figure 24: Inner Loop Step Response

From the step response:

Peak time = 0.002 seconds

Overshoot = 10 %

The design of PI Controller is not accurate since PI controller and G(s) do not match the desired transfer function, $\omega_n^2 / (s^2 + 2\xi\omega_n s)$ exactly.

3.2.4 Design of Position Controller (Outer Loop)

Step 1a: Design Criteria

The frequency of the position controller for outer loop is designed to be 10 times slower than the inner loop so that the overall transfer function is left with 1/s term (Figure 14).

Thus the design criteria are:

T_p : 0.1 second or less

% OS : 10 % step-response overshoot

The damping factor, ζ and phase margin, Φ_M are the same as before. The natural frequency, ω_n is calculated as:

$$w_n = \frac{\pi}{T_p\sqrt{1-\zeta^2}} = \frac{\pi}{0.1\sqrt{1-0.3495}} = 38.95\,\text{rad/sec} \tag{13}$$

Step 1b: Desired Open-loop Frequency Response

The desired open-loop response is:

$$G(s) = \frac{\omega_n^2}{s^2 + 2\zeta\omega_n s} = \frac{1517.27}{s^2 + 46s} \tag{14}$$

The Bode plot is:

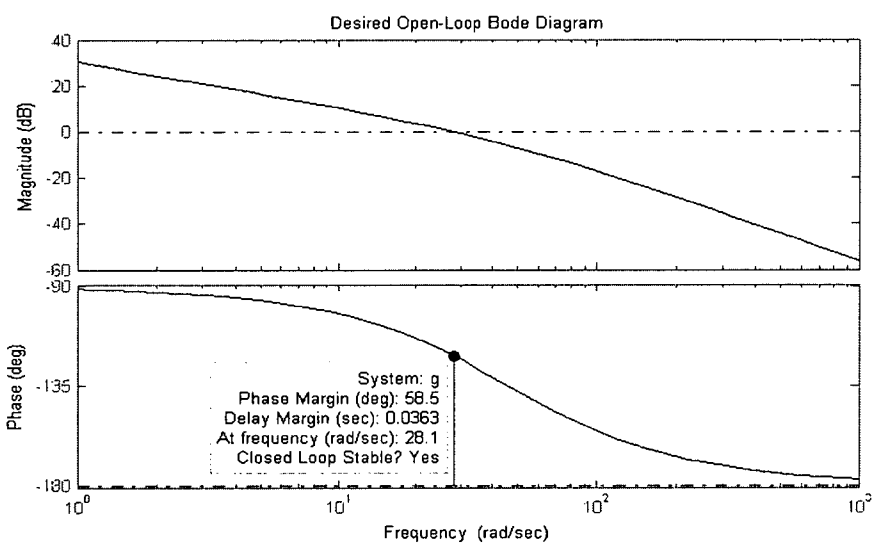

Figure 25: Desired Open-Loop Response for Outer Loop

The Desired phase margin is 58.5 deg at frequency 28.1 rad/sec.

Step 2a: Actual response with Kp = 1

The closed-loop response of 1/s with Kp = 1 is plotted as below:

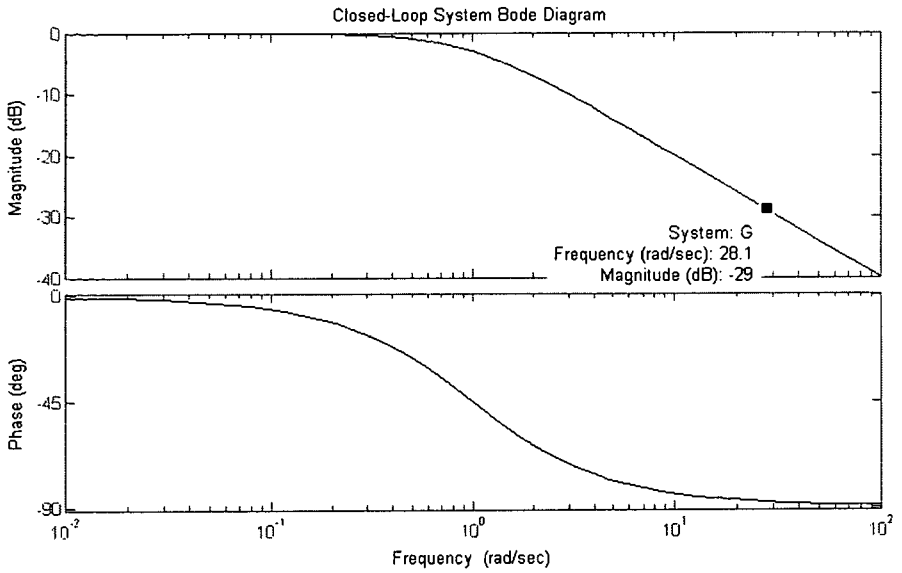

Figure 26: Closed-Loop Actual System Response (Kp = 1)

From the plot, the gain must be increased by 29 dB or $10^{(29/20)} = 28.18$.

Step 2b: Actual response with Kp = 28.18

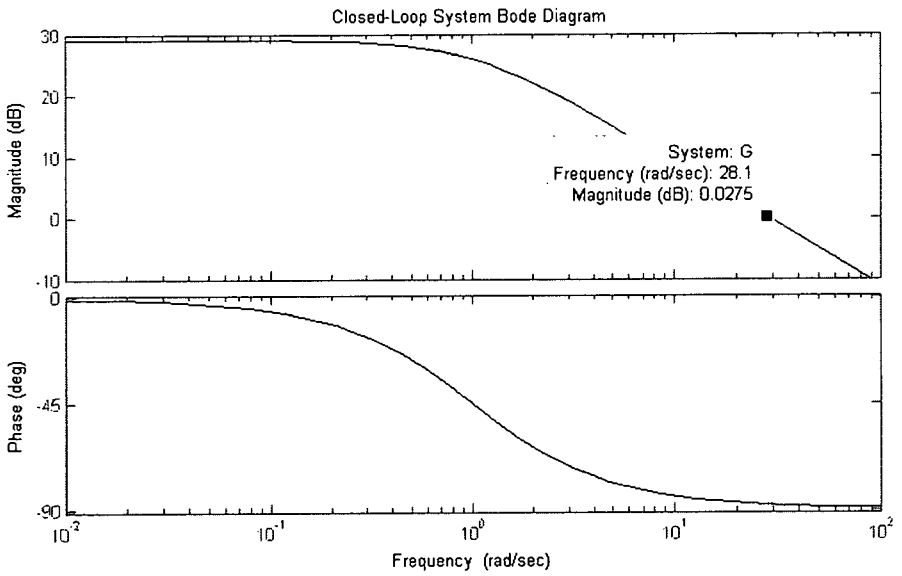

Figure 27: Closed-Loop Actual System Response (Kp = 28.18)

After increasing Kp to 28.18, the crossover frequency is now 28.1 rad/sec which is as desired.

Step 3: Verification

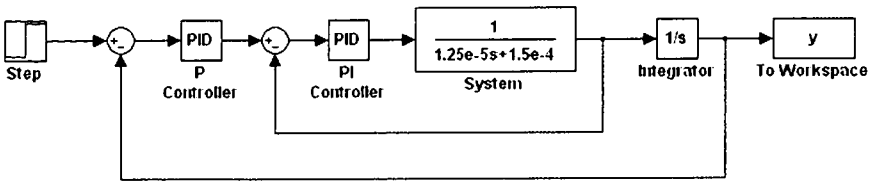

Figure 28: Simulink Verification for Overall Loop

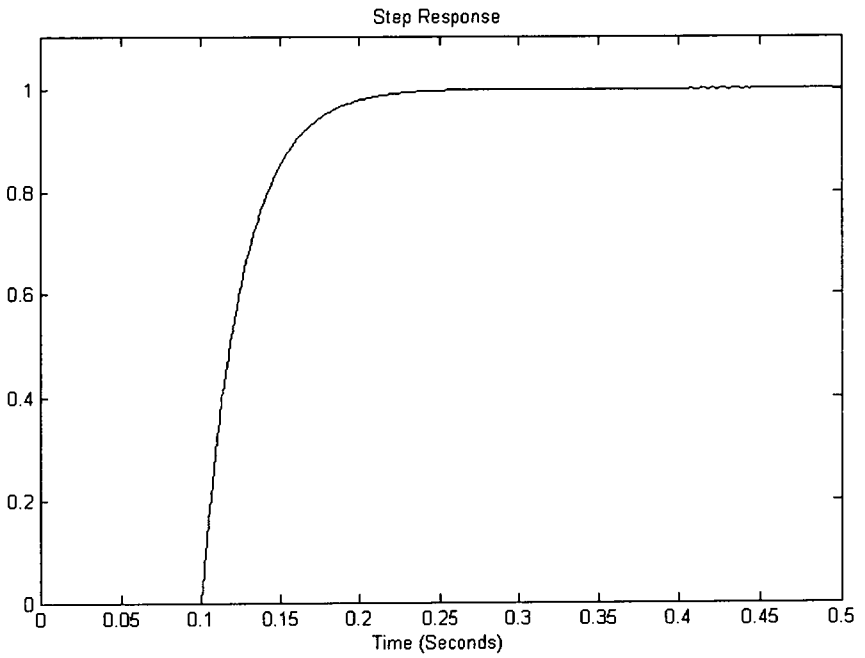

Figure 29: Overall Step Response

From the simulink verification above, it shows that the design of P and PI controller is correct. The peak time is 0.1 second with no overshoot.

The controller in Figure 26 is the complete control system for each individual manipulator.

3.3 *Coordinator and Disturbance Observer*

A precision coordination of a system is limited by the amount of disturbances present and the uniformity of the motors **[20]**. Although the motors in this system are exactly identical, it is still highly desirable for the system to be able to compensate for disturbances. These disturbances may arise from load changes or nonlinear dynamics that have not been modelled for this system such as the force ripples and frictional forces.

In order to correct for inter-position offset between the motor, a coordinator block is used which takes the difference between the current positions, x1 and x2, and passes through a P controller. The offset signal which represents a constituent control signal to correct for the inter-position offset is fed back to each individual controller.

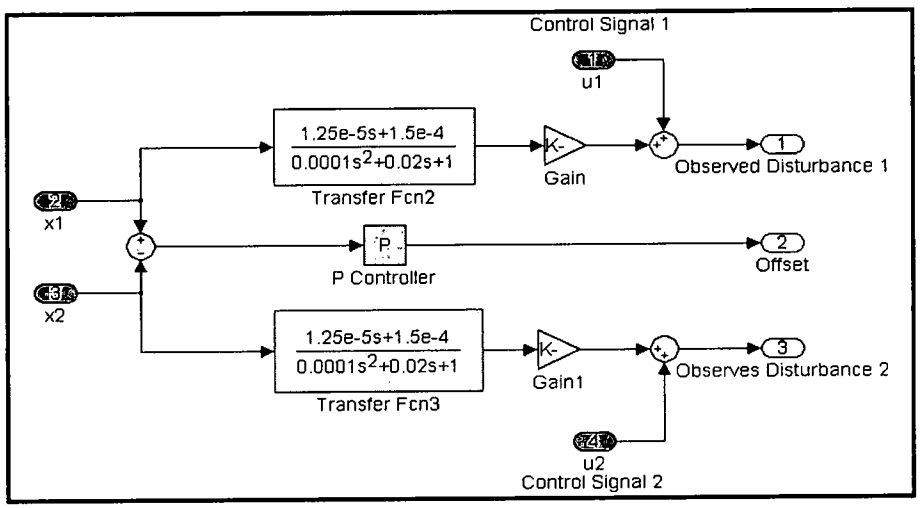

Figure 30: Simulink Coordinator and Disturbance Observer

The disturbance observer uses the output of the current motor's position (x1 and x2) which is then passed through the inverse of the system model and compared against the control signal (u1/u2). Since the inverse of the system model is used, a low-pass filter is required to make the disturbance observer practically realizable in the Simulink. The low-pass filter has the form of:

$$\frac{1}{\left(\frac{s}{100}+1\right)^2} \qquad (15)$$

The outputs from the disturbance observer (observed disturbances) are fed back to each individual control system.

3.4 Overall Coordinated Control System

Figure 31 shows the complete coordinated control system in simulink which is in the same form as the decentralized coordinated control system in Figure 13.

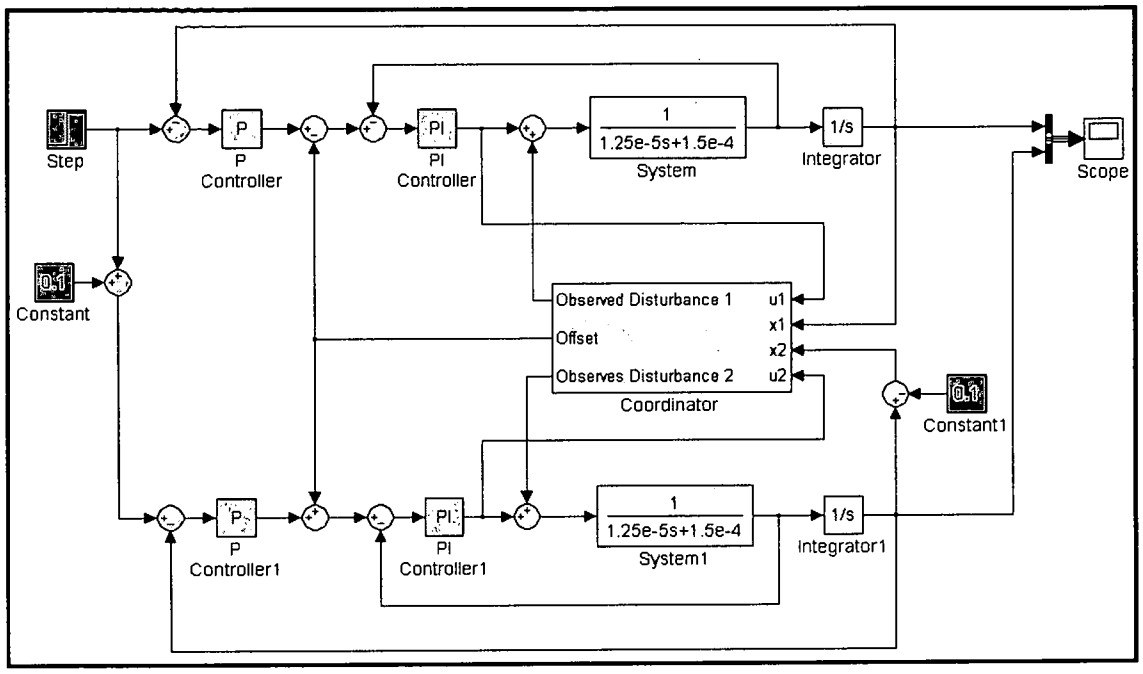

Figure 31: Simulink Overall Coordinated Control System

The control system will be simulated with a step input. The intended result to be collected from the above simulink diagram is the trajectories of each system and the inter-positional offset between their trajectories.

3.5 Simulation Results

3.5.1 Actual Trajectories of Individual Manipulator

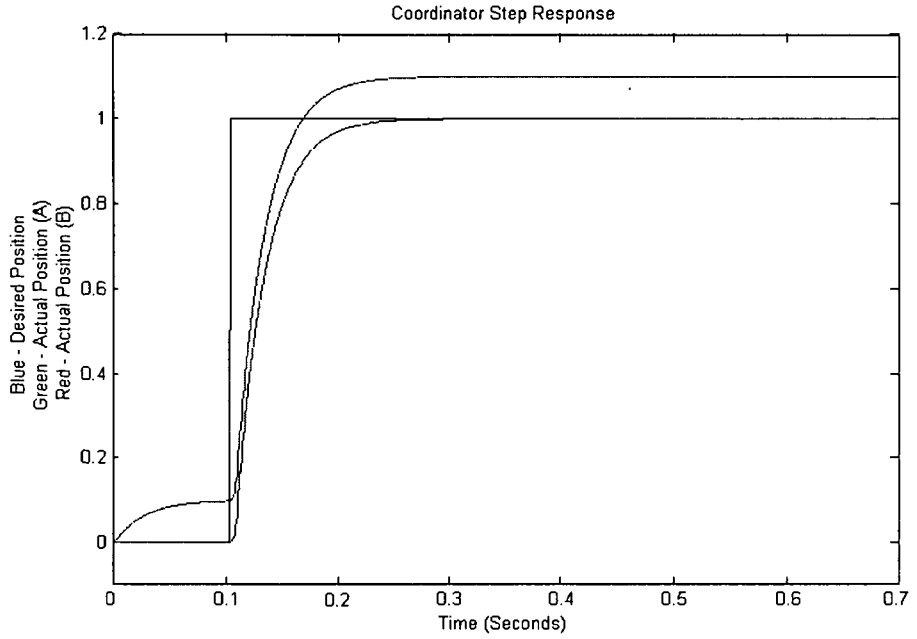

Figure 32: Simulated Actual Positions Vs Desired Position

3.5.2 Positional Offset between Manipulators

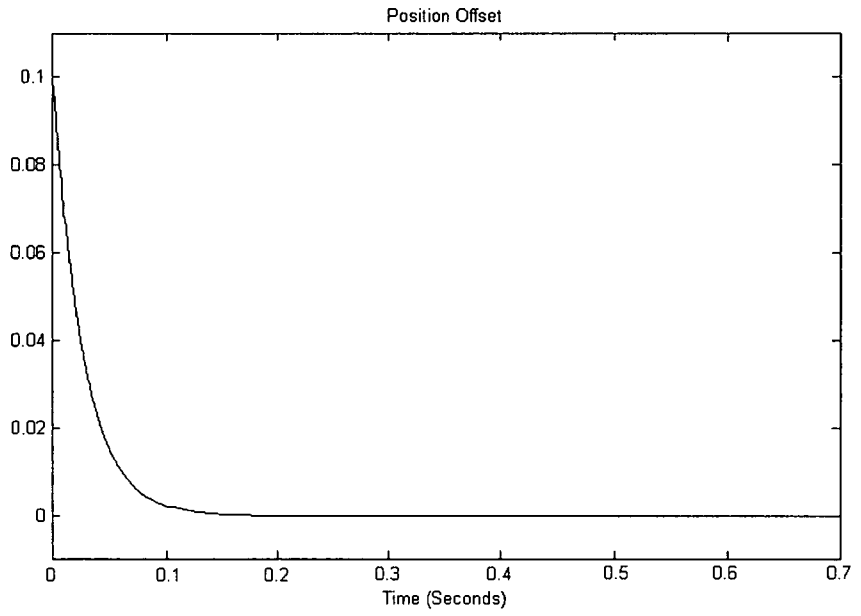

Figure 33: Simulated Positional Offset

Figure 32 shows the actual trajectories of each individual system and Figure 33 shows the inter-positional offset difference between the trajectories. The intended results from this are to have very fast responses by having a smaller settling time and rise time. This can be achieved by having a tight feedback loop for the individual controllers.

The results show that the output trajectories of the two manipulators actually tracked the desired trajectories after roughly 1.5 seconds which is slightly over than the design criteria. It can also be seen that the trajectories of the manipulators are set apart by a constant distance of 0.1. This is caused by a constant offset introduced to the second manipulator. This offset is desired since the manipulators will be attached with a string having a constant length.

As for the position offset, the maximum offset is recorded to be 0.1 at the first instant. This offset is gradually stabilized to zero after roughly 1.5 seconds.

Thus, from this simulation results, it can be concluded that the design of the coordinated control system is successful from theoretical point of view.

Chapter 4

4 Practical Implementation

4.1 Initial Configuration

Before the design of the above synchronization technique can be finalised, several self-test and parameter configurations were necessary. The first configuration was done to determine the conversion factors or the scaling needed from the motor's encoder to metres using the known gearbox, linear drive rate and revolution encoder (K1) as well as the scaling from Quanser output to the force at the linear drive (K2) as shown in Figure1.

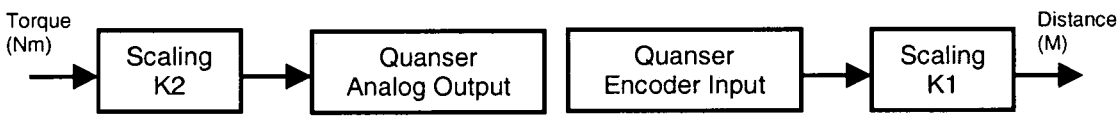

Figure 34: The scaling

The conversion factor was calculated as follows;

4.1.1 Scaling Factor K1

$$K1 = \text{encoder count} * \text{gear ratio} * \text{linear drive rate}$$
$$= 1/400 * 1/30 * 50/1000$$
$$= 5/1200$$

4.1.2 Scaling Factor K2

To calculate K2;

From Quanser voltage, V to board current, i_a:

$$i_a = k_2 * V \text{ (from measurement, } 1V = 0.094A)$$

Thus $k_2 = 0.094$ A/V

From board current, i_a to motor torque, τ:

$$\tau = k_T * i_a \text{ (from datasheet, } k_T = 55.2 \text{ mNm/A)}$$

Therefore from Quanser voltage, V to motor torque, τ:

$$\tau = k_T * k_2 * V$$

$$K2 = 1/(k_T * k_2) = 1/(55.2*10^{-3}*0.094)$$

4.2 Overview of Control system

The interface implemented for processing the signal between the control system developed in the Matlab/Simulink environment and the power boards which drive the robot's manipulator is through the Quanser Q8 DAC board (Figure 34).

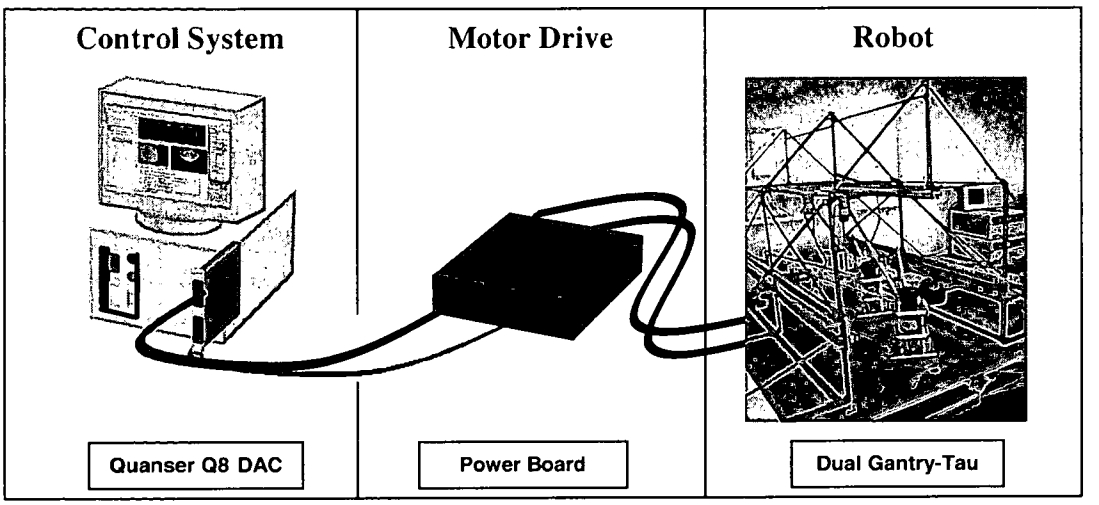

Figure 35: Overall system architecture

The Quanser board provides the necessary functional blocks in the simulink to communicate with the power boards (Figure 35). Two types of blocks are used to send and receive signals to/from the power board which are the 'analogue output' and 'encoder input' blocks. More detailed information about the Quanser board is discussed in **[12]**.

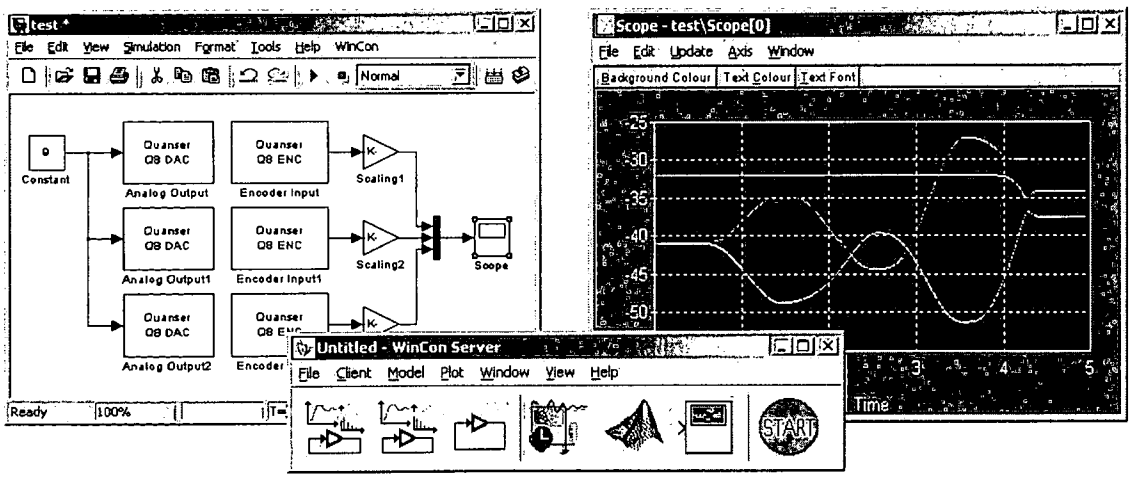

Figure 36: Quanser – Simulink Interface

4.2.1 Modification of the Actual Plan

During the initial testing phase, it was found that several control boards were faulty. There are only two control boards that are working perfectly which can only control two of the motors. Troubleshooting the faulty boards would take sometimes and it is timely to fabricate new boards. Thus, some modifications of the original plan have to be made without scarifying the project's aims. The modifications are:

- The coordinated control system will be implemented and demonstrated on two motors located on the top linear drive instead of the actual Gantry-Tau's manipulators (which are controlled by 6 motors).
- Since the motors are located on the same linear drive, there is no need for introducing the offset distance between the motors because they cannot be at the same point at the same time.
- Inverse kinematics is not needed in the system. Instead, generated trajectories (desired trajectories) can be directly used as input to the system.

These modifications do not affect the overall goal and aims of the project.

4.2.2 Generation of input signals

The identified input signals to the control system are position and velocity reference. These signals are generated in advance and saved in Matlab file. A Matlab function called *spline* is used to generate continuous input signals. The complete code can be found in Appendix section.

Below is the position and velocity reference signals used as the input to the control system:

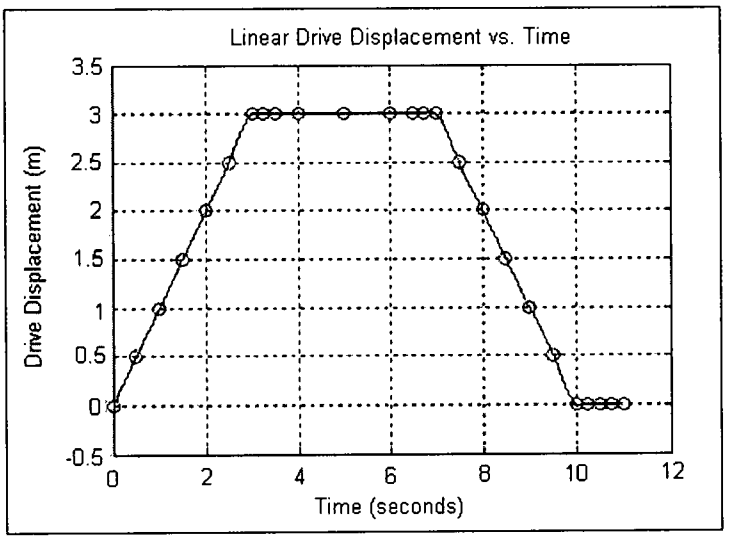

Figure 37: Position Reference

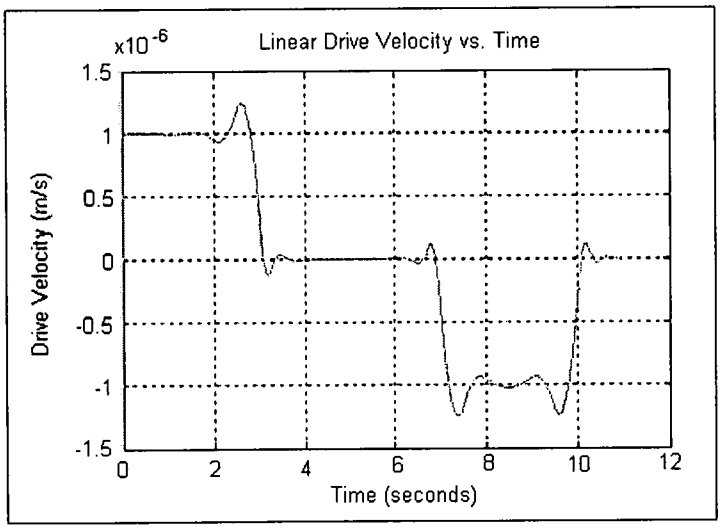

Figure 38: Velocity Reference

4.2.3 Velocity Feedback Control

In most velocity and torque controlled drive systems, closed loop control is based on measurement of velocity or position of the motor using a shaft encoder. However, in this system there is no speed sensors incorporated into the design. The strategies is to estimate the motor velocity and used as feedback signal for closed-loop velocity control. This is done by feeding back the position output through a low pass filter as shown below:

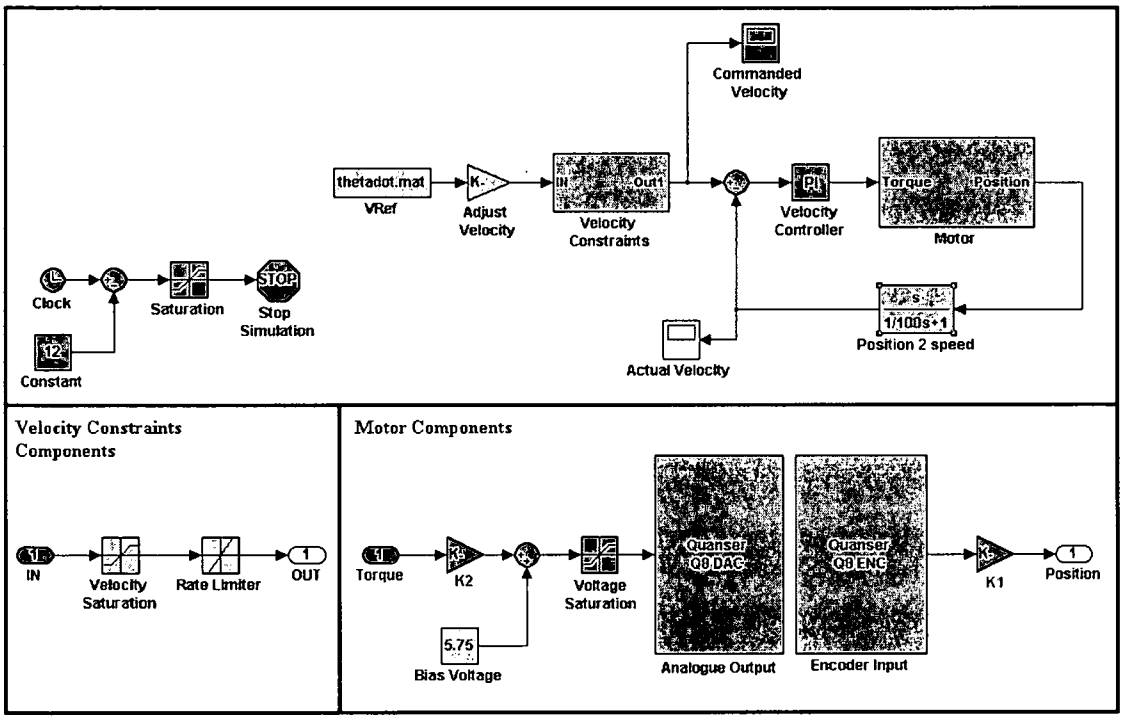

Figure 39: Velocity Feedback Loop

A generated velocity reference is given as the input to the system. This is then passed through a velocity constraint block which contains velocity saturation to limit input signal to lower and upper saturation values and rate limiter to limit input rising and falling rates.

The analogue output block in the motor components takes a 0-10 volts signal from the model and outputs this value to the Quanser board analogue port. A saturation block was used to limit signals to this range. A 5.75 volts bias is required by the power boards for the motor direction midpoint. This means that the Quanser output ports are configured to hold a voltage at 5.75 volts to enable to the motors to be held at stationary when no control signal is present.

4.2.4 Position Feedback Control

The position feedback control was achieved by simply adding the position control loop outside the velocity loop as shown in Figure 39 below. The input to this position closed-loop control is the generated position reference as described earlier.

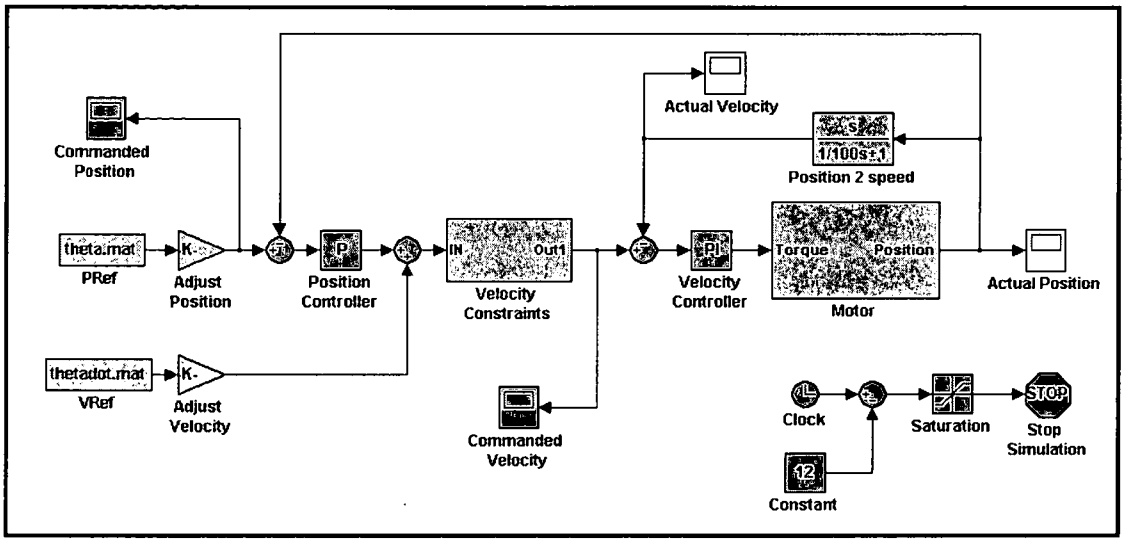

Figure 40: Position Feedback Control

Control of the position was achieved by only using a P controller to speed up the response. The transient effects such as overshoot are already reduced by the inner closed-loop control of the velocity.

Figure 39 above shows the complete control system which is used for individual motor in practical.

4.2.5 Coordinator and Disturbance Observer

Practically, the damper, having a form of Ds, is found to be useful to minimise the spring effect of having the P controller alone in the coordinator block. This is evidenced from the coordinator output with and without the damper as shown below:

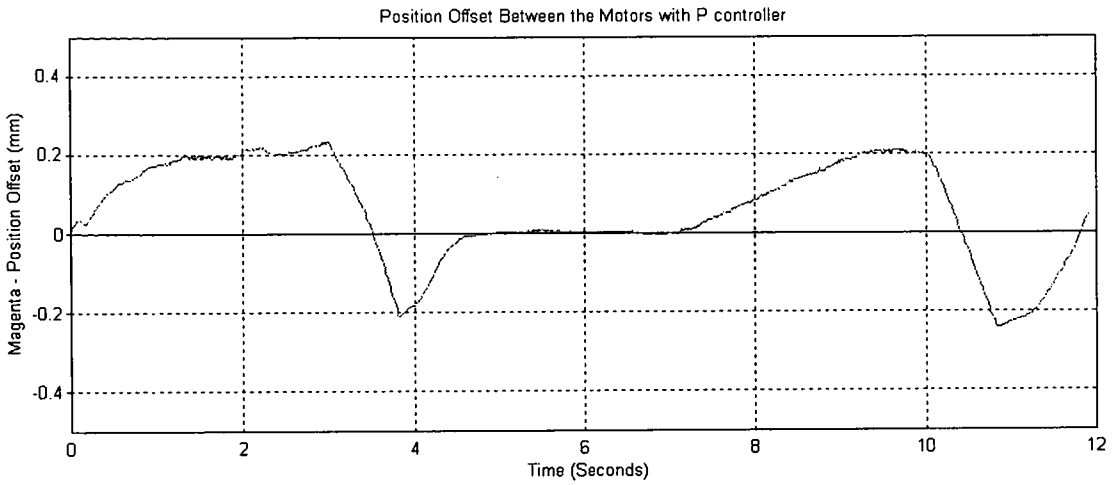

Figure 41: Position offset with P Controller

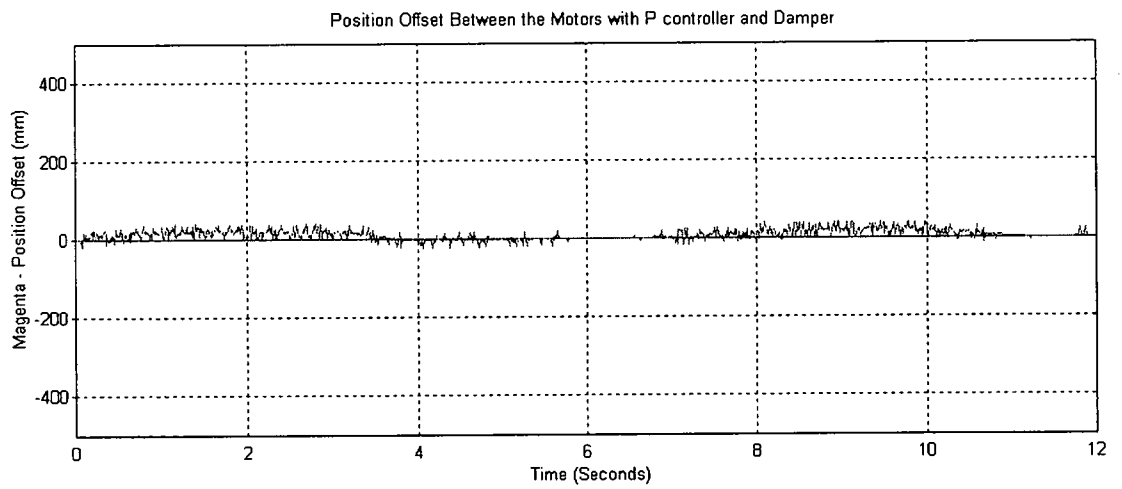

Figure 42: Position offset with P Controller and Damper

After the damper in introduced in parallel with the P controller, the response is more stabilized.

Figure 43 shows the block diagram of the coordinator with the damper in parallel with the P Controller and disturbance observer which is part of the overall control system for the Gantry-Tau.

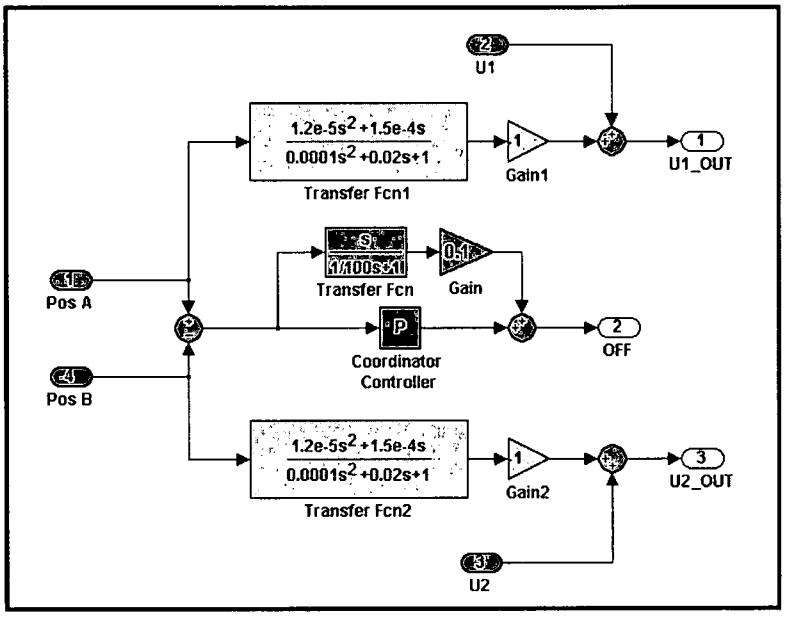

Figure 43: Practical Coordinator and Disturbance Observer

In practical observation, it is found that the damper with the same value as the P controller in the coordinator gives the optimal results.

4.3 The Complete Control System

The complete coordinated control system for the Gantry-Tau is depicted in Figure 44 below:

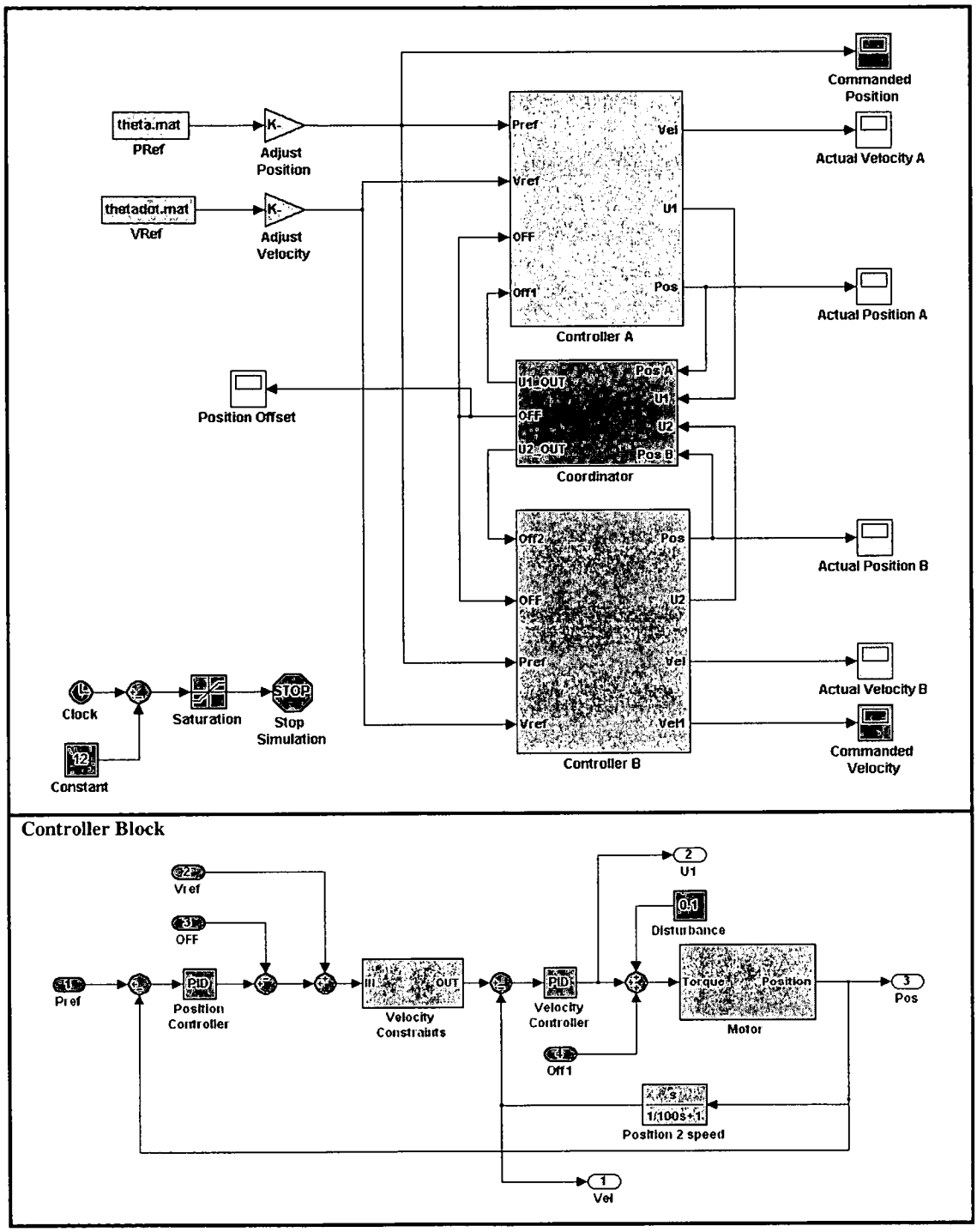

Figure 44: The Complete Control System

Chapter 5

5 Results

In this chapter experimental results will be illustrated in graphical forms. The intended results are the actual position and velocity responses of each motor as well as the positional offset between the motors. The initial gain parameters used in the experiments are:

PI velocity controller: P = 2, and I = 4

P position controller = 2.5

P coordinator controller = 0.1

Damper = 0.1

Five experimental cases have been carried out having different set of configurations as explained below:

Case A: The control system is run under normal condition with 0 disturbances. Only the coordinator is used without implementing the disturbance observer yet.

Case B: The control system is run with simulated disturbance of 0.1 introduced at motor A. As in case A, the system only incorporates the coordinator without the disturbance observer.

Case C: As in case B. At this time the P controller and the damper in the coordinator are increased to 1.

Case D: As in case B but with the disturbance observer implemented in the control system.

Case E: As in case D. The P controller and the damper in the coordinator are increased to 1.

The results from each case will be compared against the performance criteria. Effectiveness of the control system for each case will be evaluated and discussed in section 6.

5.1 Case A: Ideal Condition

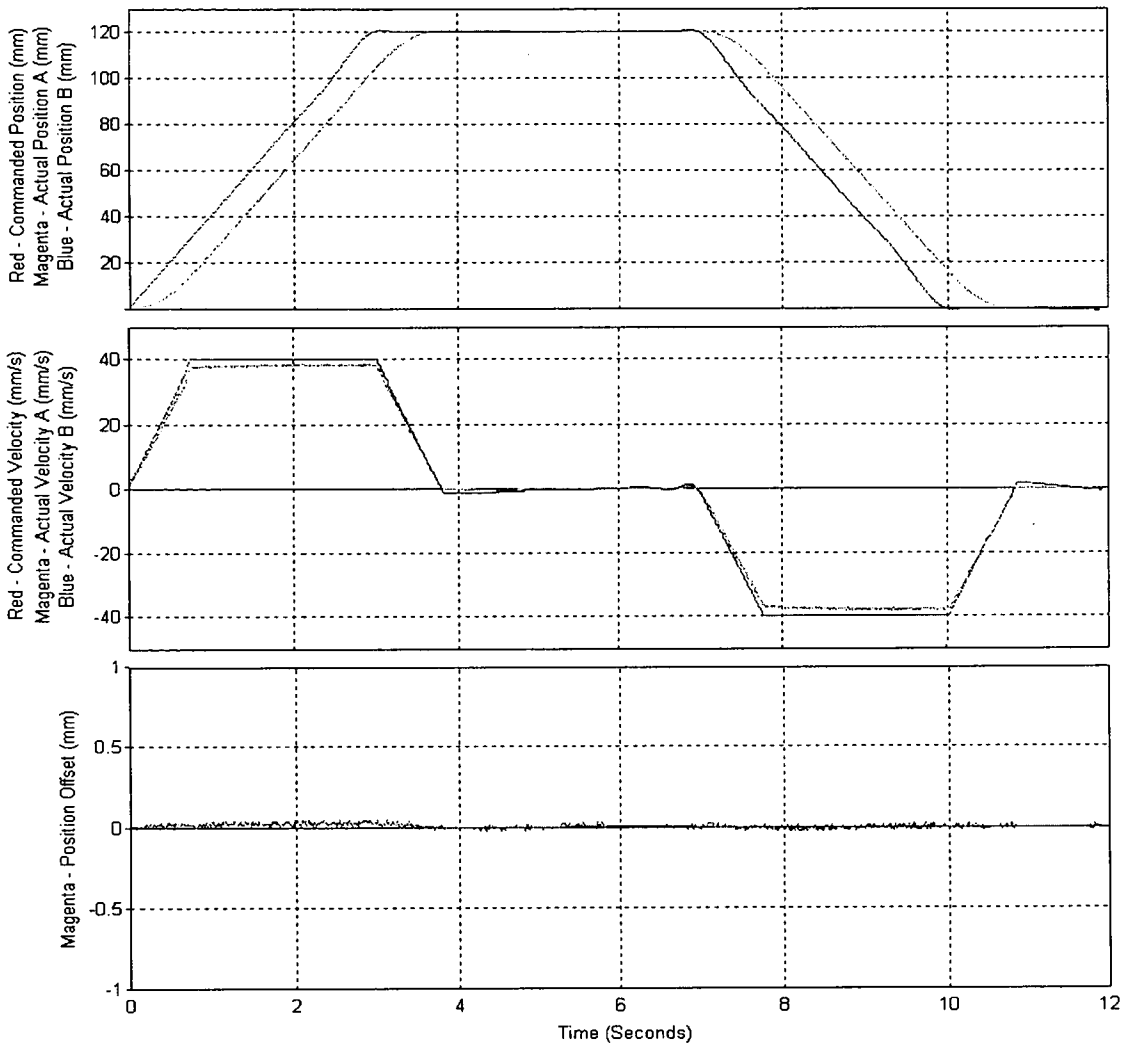

Figure 45: Results for Case A

From the top graph, it is evidenced that precision movement of each motor to track the desired position is achieved but with a 0.5 second delay. This delay is insignificant since the desired performance is to reach the 12mm displacements as commanded to the motors. The velocity response is as desired as can be seen from the middle graph. It is also proved that the inter-positional offset between the motors is stabilized and maintain at zero.

5.2 Case B: Disturbance at Motor A

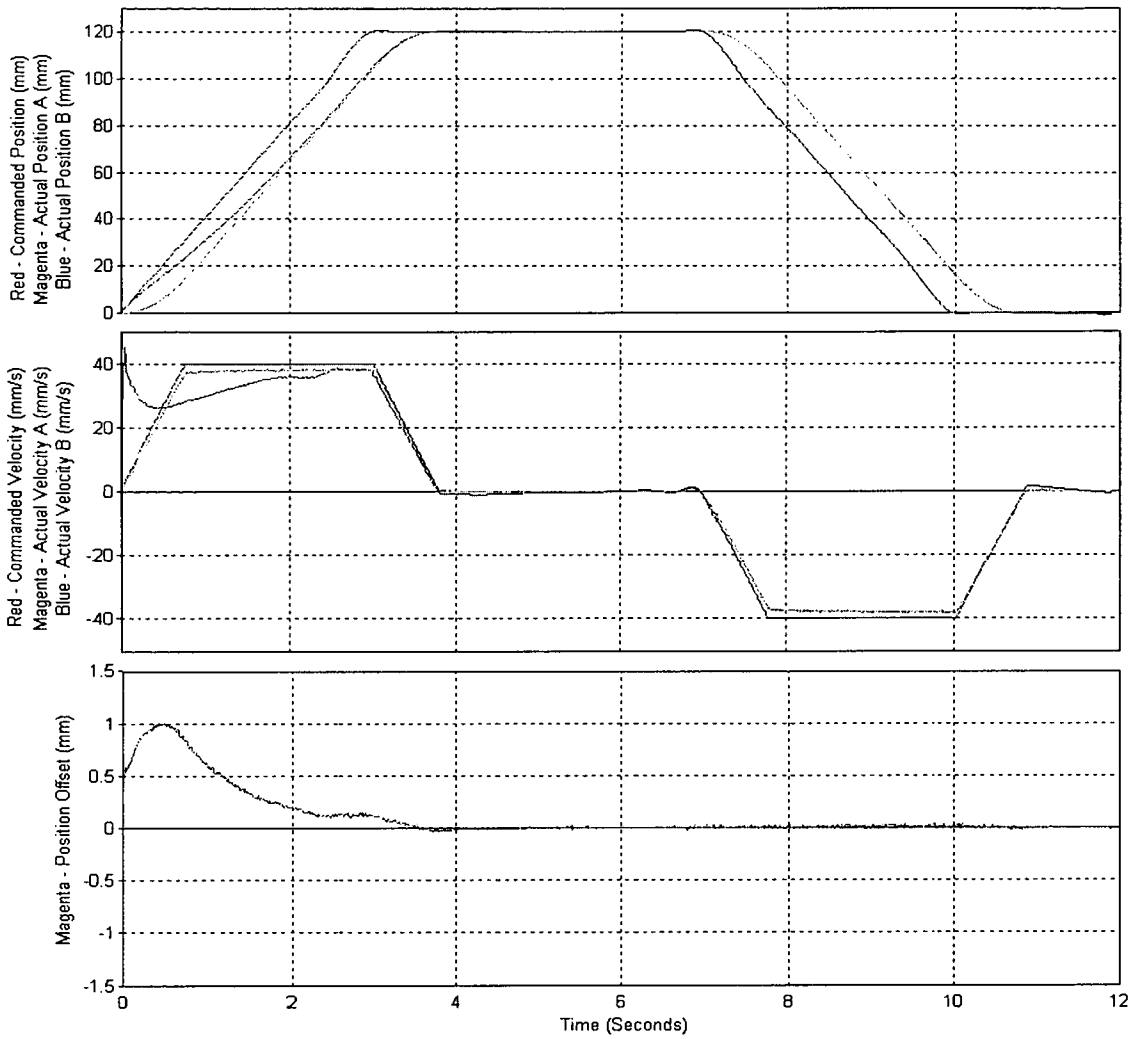

Figure 46: Results for Case B

In this case, disturbances are given at motor A alone to simulate an actual disturbance that might be experienced by the system in real. As the disturbance is given to motor A, the position and velocity responses of motor A are interrupted during the first 3 seconds. However, the control system was able to manage these disturbances and stabilized this error. The initial inter-position offset error is 1 mm. For small value of disturbances (i.e. 0.1) the offset of 1mm is significant and thus it not desirable for the system.

5.3 Case C: Optimising the Disturbance Control

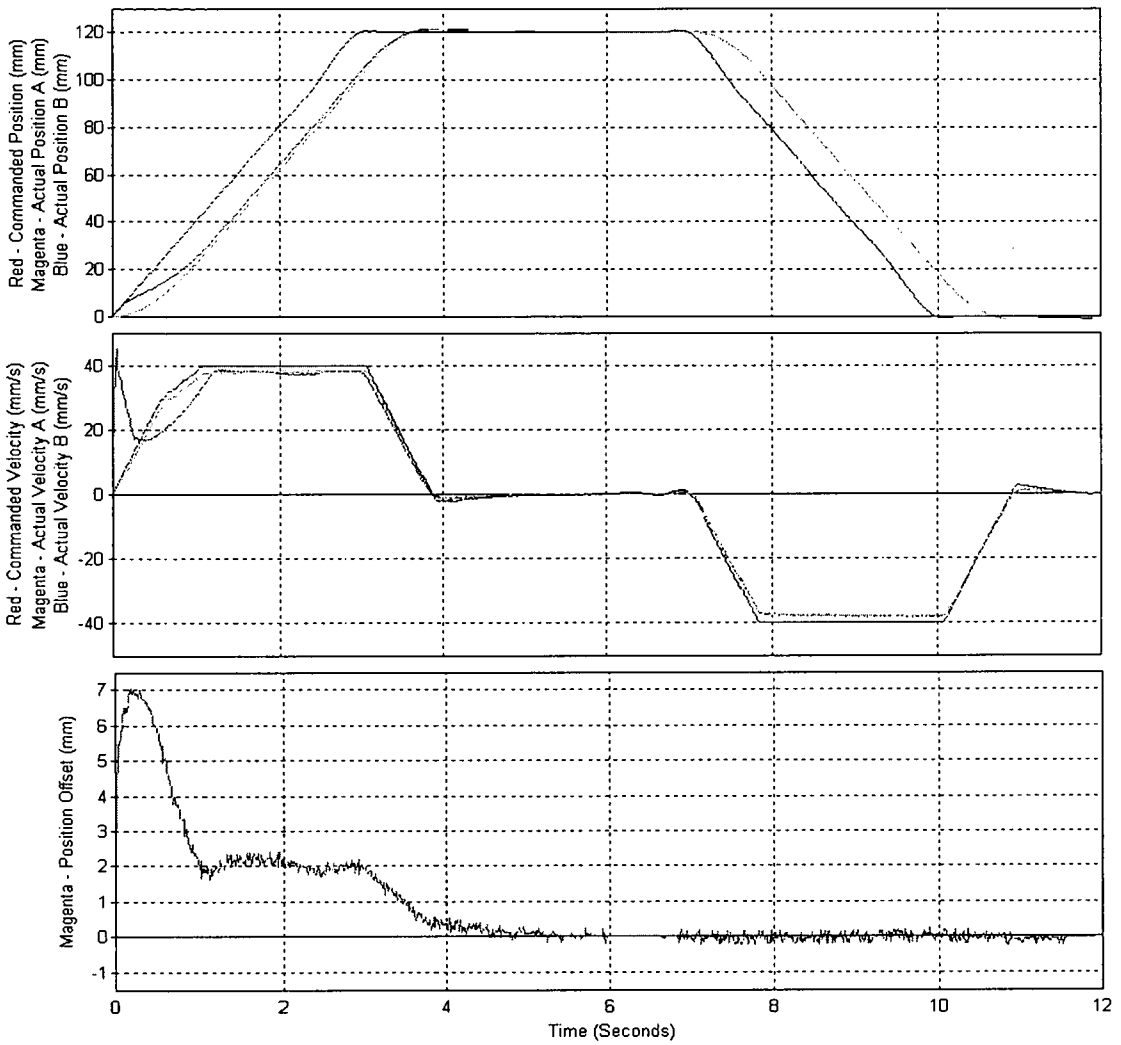

Figure 47: Results for Case C

In this case, the coordinator parameters are increased hoping that this will compensate for the disturbances. From the responses above, the improvement is not significant. Besides, by increasing the controller gain, the offset is increased to 7 mm reflecting the poor inter-position coordination. Apparently, it also amplified the noise in the system. Apart from that, sudden changes in velocity output is also observed during the first second which is undesirable.

5.4 Case D: Disturbance Observer

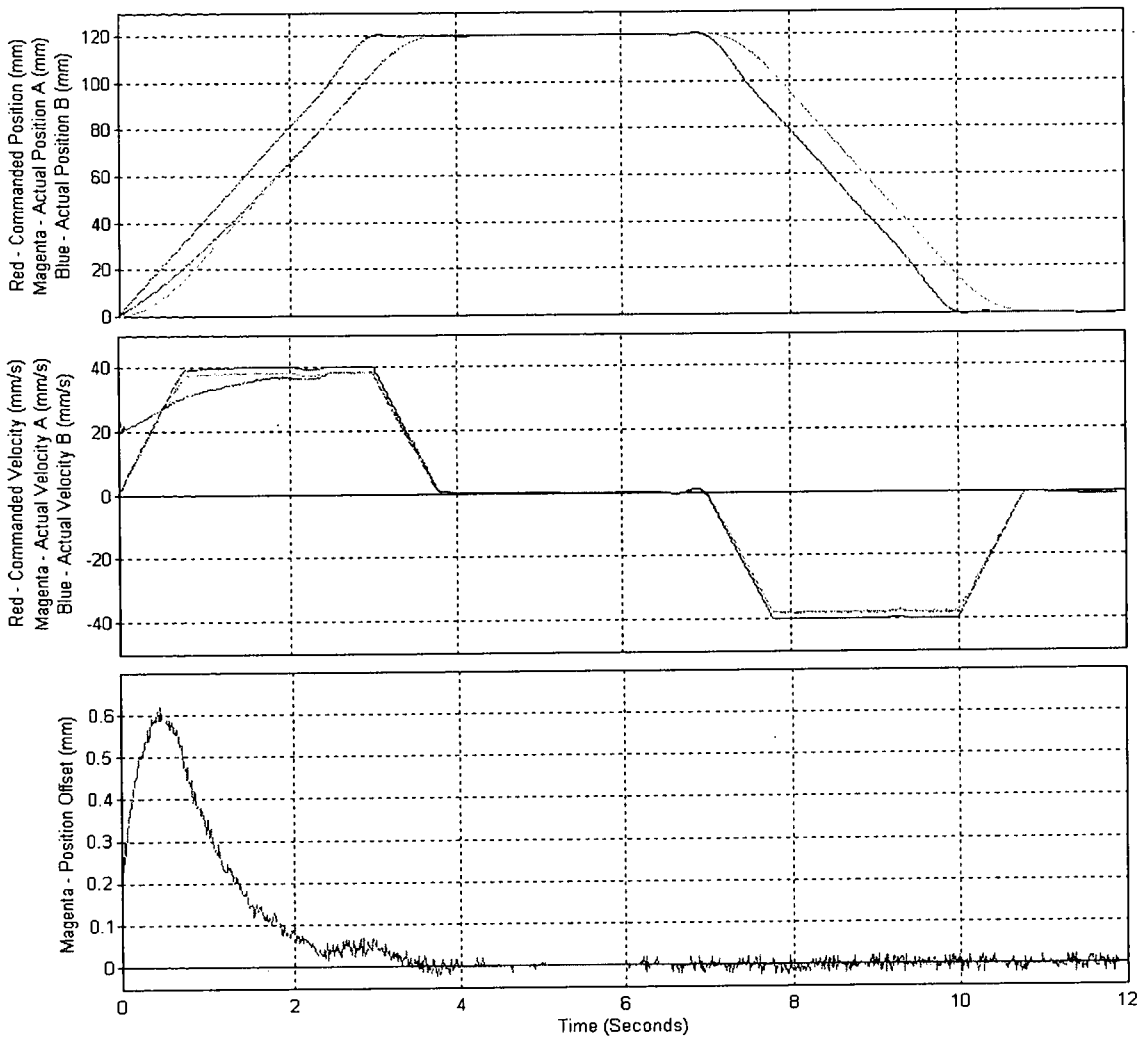

Figure 48: Results for Case D

Under the disturbance observer control system, experimental results show that the velocity output of motor A is well controlled. The inter-position offset between the two motors is 0.6 mm, which is better than case B.

5.5 Case E: Optimising the Disturbance Observer

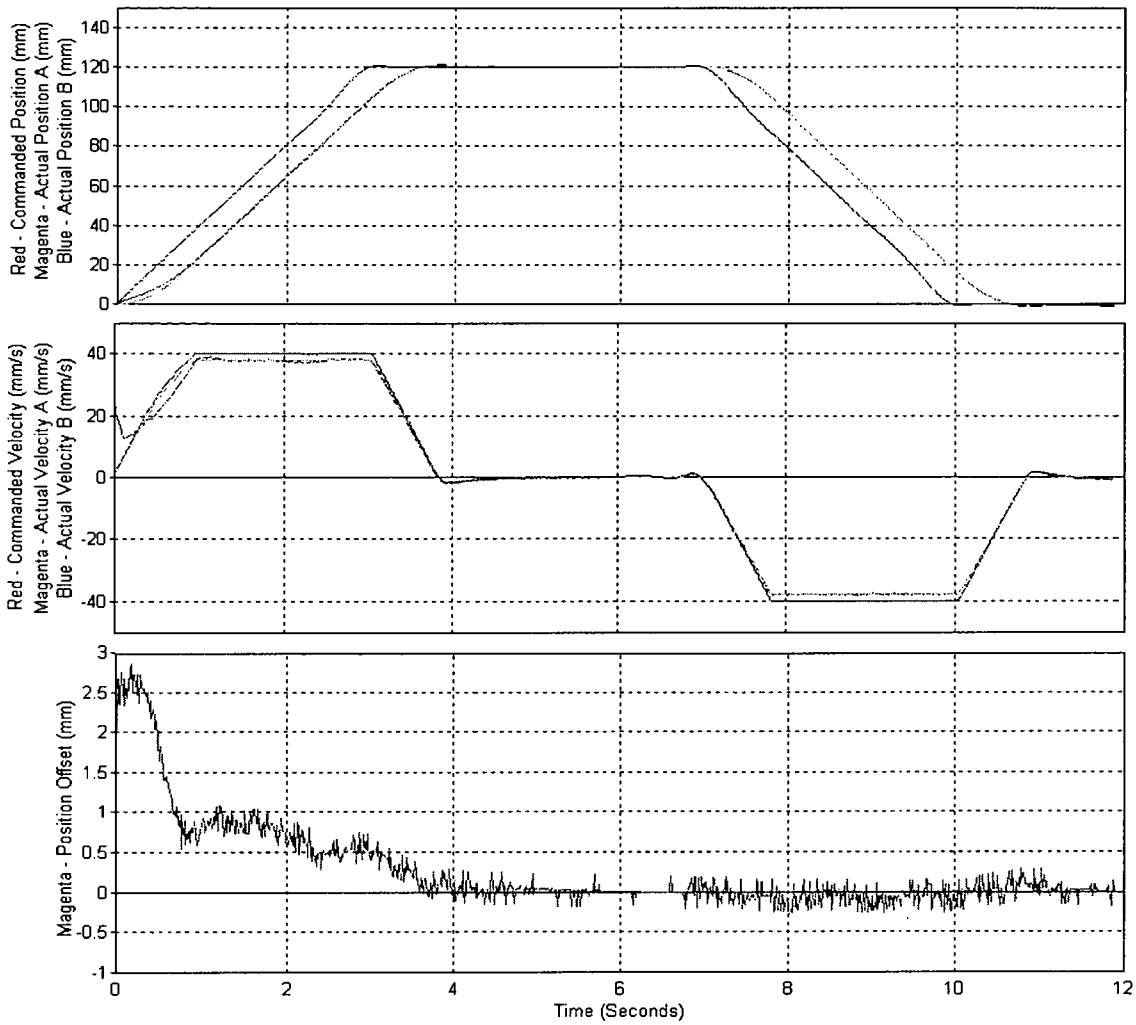

Figure 49: Results for Case E

Optimising the coordinator parameters in case D resulted in better control of the velocity. Unfortunately, as in case C it also has the effect of increasing the offset and amplifying the noise in the system. However, the recorded offset was 2.5 mm which is still tolerable.

Chapter 6

6 Discussion and Critical Review

The purpose of this chapter is to illustrate the success of the project with respect to the project's aims outlined in chapter 1.2. The criteria used for evaluation of each result are specified and discussed accordingly.

6.1 The System Model

The system model developed in section 3.2.1 gives the estimated transfer function of the Dual Gantry-Tau PKM. This transfer function is required to design the controller's parameters for individual control system. An important factor that affecting the accuracy of the transfer function is heavily depending on the simplifications made when modelling the motor. Furthermore, the estimation was done from the graph of position response which could lead to further errors.

The correctness of the system was roughly estimated by comparing the values of $J + mr^2$ and d with system identification done in [26] for the Gantry-Tau PKM developed in 2004 by [12]. However, this comparison is inaccurate since some variations exist between the two PKMs especially the motor specifications. Thus, the modelling of the system has to be improved in the future for better control system design.

6.2 Simulation Results

The design of position and velocity controller was done by the frequency analysis techniques using the Bode plots. Bode plots are very useful in designing or analysing a control system since the effect of adding poles and zeros can be seen rather easily.

The design of PI Controller is not quite accurate since PI controller and G(s) do not match the desired transfer function, $\omega_n^2 / (s^2 + 2\xi\omega_n s)$ exactly. As with the position controller, it is fairly accurate since the design only incorporates a simple P controller. Overall, the simulation shows promising results for successful practical implementation of the coordinated system for the Dual Gantry-Tau.

6.3 Experiment Results

Several different experiments were conducted in order to confirm that the design work properly as expected and to evaluate the system behaviour at different conditions. From the results, it can be concluded that with the present of disturbances, optimising the coordinator controller did not promise a better result unless the system has the ability to observe the react to the disturbances accordingly. Thus, the disturbance observer incorporated together with the coordinator plays a major role in compensating the disturbances.

In practical, the optimal controller parameters used for the velocity and position control are:

Velocity controller: P = 2, I = 4

Position Controller: P = 2.5

The discrepancies in the simulation and experiment results can be attributed to the simplification made when modelling the system.

The results gained from the experiments are positive and show that the methods of decentralized control proposed for the Dual Gantry-Tau has great potential.

6.4 Evaluation of Project

It is necessary to evaluate the planning of the project and the decisions that have been made throughout the project. This will provide feedback on whether the assumptions made at the start were correct and valid as well as whether the actions and decisions made throughout the project were correct and justified. The ultimate aim of an evaluation is to ensure success for future projects and to avoid the same mistakes.

6.4.1 Project's Goals

In general, the initial project's goal outlined in section 1.2 was achieved with a slight modification made to the Dual Gantry-Tau. The initial plan was to fully control both of the Gantry-Tau arms. In order to do this, it needs 6 control boards that are working properly. However, 4 of the control boards that were originally build for the Gantry-Tau are faulty. Since there was not enough working control board available, the plan was changed to only control two of the Gantry-Tau motors. Apart from this change, the demonstration of the coordinated control system was made possible.

6.4.2 Project's Schedule

The project schedule is fundamental to the project and if followed, should lead to the completion of the project. This, of course, is provided that it is properly constructed and is reviewed and evaluated regularly.

The initial project schedules (Figure 53 and 54) were made concisely to fit the duration of one semester and correct based on the assumptions made at the beginning of the project. Unfortunately, the time spent on troubleshooting the faulty boards (initially not scheduled in the Gantt chart) took about 2 weeks which pushed back the rest of the project. Therefore, some of the lab works have to be done outside the normal working times and some of the project scopes have to be limited. This is the challenge of one semester project where every time has to be managed efficiently.

6.4.3 Risk Management

The potential risks that might present in this project were not adequately defined at the earlier project stage. The risk that the control boards were not working did not fully eventuate until all possible testings and implementation were tried.

The most important lesson learnt from this is, it is critical to identify the risks earlier in the project to avoid any delay. A time limit should have been set such that if the control boards were not working by that date, then it would be abandoned and the focus would be moved elsewhere.

Chapter 7

7 Conclusions

7.1 Project Outcomes

The focus of the thesis was to design a coordinated control system that could precisely synchronize the motion of two Gantry-Tau robot manipulators for the purpose of application in industries. An overview and comparative study of the Gantry-Tau robot has been presented in this thesis together with several other Parallel Kinematic Machines of its kind. In order to develop the control system, a thorough evaluation of the currently available coordinated control schemes was conducted in terms of their advantages and disadvantages.

Although there are many control techniques available, extra effort had to be made in choosing the best control technique for the Gantry-Tau. One such area requiring urgent attention was to decide the appropriate control technique that would fit the specific applications intended for the Gantry-Tau, performance requirements and the current Gantry-Tau architecture. The results from the evaluation of the current control system were used together with these criteria to identify the final coordinated control technique to be implemented in this project. In response to this, the positive traits of a decentralized coordinated control scheme were identified and its features were used to realize the project's goal.

The crucial part in this project was implementing the technique on the real system. Before the implementation was done a significant problem was encountered regarding the control board. Thus the consequence of the board troubleshooting was continual delays of the project during the last five weeks. However apart from this problem, the project aim was successfully achieved with some modifications of the original goals. The control system was implemented on two motors located on the top linear drive instead of the actual Gantry-Tau's manipulators which are controlled by 6 motors. This is sufficient to demonstrate the reliability of the control system design.

7.2 Contributions

This thesis has presented issues related to a coordinated control system particularly in methods for motion synchronising.

It has examined some of the existing techniques for ensuring motion coordination in great detail. From the evaluation it has been found that the best control technique is the decentralized coordinated control architecture. The advantages of this method are simple arrangement and more straightforward application. The coordination can be achieved with only position control without explicitly employing internal force controls. Another benefit of this scheme is stability of position and synchronization errors guaranteed as deficiencies of one robot do not directly affect the other robot. The effectiveness of this method through individual feedback control and differential position error feedback allows the Gantry-Tau to maintain a high level of control. This is proved to be valid through experimental verification.

Apart from coordination control, this thesis also presented methods for disturbance control with the implementation of disturbance observer. The observer can be used to model external disturbances to the system such as the weight of workload carried by the motors. This additional feature provides a basic platform for more robust control of the Gantry-Tau and can be further utilized and strengthened in the future.

7.3 Future Improvements

The coordinated control system built in this project is still far from perfect. There is a lot of room for further improvement in many aspects with regards to the current status of the project. Due to the time constraints of this project, its scope was limited to only developing a reasonably working coordinated control for two of its motors. There was an insufficient time to implement all aspects of a fully coordinated control system which includes path planning and collision avoidance. Due to this the full potential of the Gantry-Tau system could not be explored. However, the work completed has shown the potential benefits and feasibility of these systems. This approach can be further strengthened through the following extensions:

7.3.1 System Modelling

The estimation of the system model was very basic and thus may represent a significant inaccuracy. Since the derivation of the system's transfer function was based on the position time response, it is essential to perform the experiment practically properly with the data recorded properly. This area requires further work by applying more reliable system identification methods. It is also crucial for modelling works to go through various iteration processes for better system parameters optimization which leads to a high performance control system.

7.3.2 Fully coordinated control of Gantry-Tau System

For better realization of the dual Gantry-Tau adaptability, a fully coordinated control system of its manipulators is desired. This needs time to be spent on the current control boards that are faulty or fabricating new control boards. With the possibility of a fully coordinated control system, there is great potential for future projects to carry on this work concentrating on the following aspects:

7.3.2.1 Integration of path planning

Autonomous control of Gantry-Tau can be achieved through integration of path planning using the inverse kinematic which was established well in advance. This involves constant re-evaluation of the current position of each tool point.

7.3.2.2 Optimization of task sharing and collision avoidance

The possibility of significant optimization with relation to task sharing between the two tool points can be achieved by having each tool point operate at each ends of a work piece. Thus significant gains can be made where both tool points cooperate to achieve a task. This means that the Gantry-Tau could carry a heavier load or perform assembly operations that require different orientations of the work piece. Dealing with the possibility of link or drive collisions was not explicitly covered in this project. Although for automated tasks the path planning can be done well in advance, it is still crucial to integrate safety protocols to avoid collisions.

7.3.2.3 Strategies for switching between synchronized and unsynchronized motions

As mentioned in 2.2.3, this project primarily focussed on the development of coordinated control system for type 2 only. The question of how to extend the control system to accommodate both type 1 and type 2 system needs to be addressed. The ability of Gantry-Tau to perform both synchronized and unsynchronized motions interchangeably is highly desirable.

References

[1] Staicu, S. and Carp-Ciocardia, D. C. (2003). Dynamic analysis of Clavel's DELTA parallel robot. *Proceedings of the 2003 IEEE International Conference on Robotics & Antomation, Taipei, Taiwan,* 4116-4121.

[2] Tan, T. J., Bejczy, A. K. and Yun, X. (1986). Coordinated control of two robot arms. *Proceeding of the IEEE International Conference on Robotics and Automation,* 1193–1202.

[3] Berghauser, M. (2005). Build a destop sized parallel robot. Undergraduate Thesis for the ITEE Department at the University of Queensland, Brisbane, Australia.

[4] Carp-Ciocardia, D. C and Staicu, S. (2005). Dynamics of DELTA parallel robot with prismatic actuators. *Proceedings of the 2005 IEEE International Conference on Mechatronics, Taipei, Taiwan,* 870-875.

[5] Codourey, A. (1996). Dynamic modeling and mass matrix evaluation of the DELTA parallel robot for axes decoupling control. *Proceeding of the 1996 IROS, 1211-1218.*

[6] Miller, K. (1995). Experimental verification of vodeling of DELTA robot dynamics by direct application of Hamilton's principle. *IEEE International Conference on Robotics and Automation,* 532-537.

[7] Pierrot, F., Fourneir, A. and Dauchez, P. (1991). Towards a fully parallel 6 DOF robot for high speed applications. *Proceedings of the 1991 IEEE International Conference on Robotics & Antomation, Sacramento, California,* 1288-1293.

[8] Pierrot, F. and Company, O. (1999). H4: a new family of 4-dofparallel robots. *Proceedings of the 1999 IEEE/ASME International Conference on Advanced Intelligent Mechatronics, Atlanta, USA,* 508-513.

[9] Company, O., Marquet, F. and Pierrot, F. (2003). A New High-Speed 4-DOF Parallel Robot Synthesis and Modeling Issues. *IEEE Transactions on Robotics and Automation,* **19**(3): 411-420.

[10] Hervé, J. M. and Sparacino, F. (1991). Star, a new concept in robotics. *3rd International Workshop on Advanced in Robot Kinematics, Ferrara, Italy,* 176-183.

[11] Brogårdh, T. (2002). Pkm research - important issues, as seen from a product development perspective at ABB robotics. *Proceedings of the Workshop on Fundamental Issues and Future Research Directions for Parallel Mechanisms and Manipulators,* Quebec, Canada, 68-82.

[12] Murray, M. (2004). Building a prototype parallel robot. Undergraduate Thesis for the ITEE Department at the University of Queensland, Brisbane, Australia.

[13] Johannesson, L., Berbyuk, V. and Brogårdh, T. (2002). Gantry-Tau – A New Three Degrees of Freedom Parallel Kinematic Robot.

[14] Hovland, G., Brogårdh, T. and Murray, M. (2006). A new friction and dynamic model of the 3-DOF triangular Gantry-Tau parallel manipulator. *Submitted for review to the IEEE Transaction on Robotics.*

[15] Tremblay, A. and Baron, L. (1999). Geometrical synthesis of star-like topology parallel manipulators with a genetic algorithm. *Proceedings of the 1999 IEEE International Conference on Robotics & Automation*, 2446-2451.

[16] Choi, H. B., Company, O., Pierrot, E., Kono, A., Shibukawa, T. and Uchiyama, M. (2003). Design and control of a novel 4-DOFs parallel robot H4. *Proceedings of the 2003 IEEE International Conference on Robotics & Automation, 1185-1190.*

[17] Nabat, V., De La O Rodriguez, M., Company, O., Krut, S. and Pierrot, F. Par4: very high speed parallel robot for pick-and-place.

[18] Miller, K. (2002). Maximization of Workspace Volume of 3-DOF Spatial Parallel Manipulators. *Journal of Mechanical Design, 124: 347-357.*

[19] Sun, D and Mills, J. K. (2002) Adaptive synchronized control for coordination of multirobot assembly tasks. *IEEE Transactions on Robotics and Automation,* **18**(4): 498-510.

[20] Tan, K. K., Lim, S. Y., Huang, S., Dou, H. F. and Giam, T. S. (2004). Coordinated motion control of moving Gantry stages for precision applications based on an observer-augmented composite controller. *IEEE Transactions on Control System Technology,* **12**(6): 984-991.

[21] Wen, J. T. and Delgado, K. K. (1992). Motion and force control of multiple robotics manipultors. *Automatica*, **28**(4): 729-743.

[22] Wang, J., Dodds, S. J. and Bailey, W. N. (1997). Co-ordinated control of multiple robotic manipulators handling a common object – theory and experiment. *IEE Proceeding on Control Theory Application*, **144**(1): 73-84.

[23] Yoshikawa, T., Sugie, T. and Tanaka, M. (1988). Dynamic hybrid position/force control of robot manipulators-controller design and experiment. *IEEE Journal of Robotics and Automation, 4(6): 699-705.*

[24] Tan, T. J., Bejczy, A. K. and Yun, X. (1986). Coordinated control of two robot arms. *Proceeding of the IEEE International Conference on Robotics and Automation,* 1193–1202.

[25] Liu, Y., Arimoto, S. and Ogasawara, T. (1996). Decentralized Cooperation Control: Non-Communication Object Handling. *Proceeding of the IEEE International Conference on Robotics and Automation, Minnesota,* 2414-2419.

[26] Gunnar, J., Wernholt, E., Hovland, G. and Brogardh, T. Nonlinear grey-box identification of linear actuators containing hysteresis.

[27] Nise, N. S. (2003). *Control Systems Engineering.* Third Edition, John Wiley & Sons

Appendixes

A: Motor Specifications

F 2140 ∅40 mm, Graphite Brushes, 6 Watt, CE approved

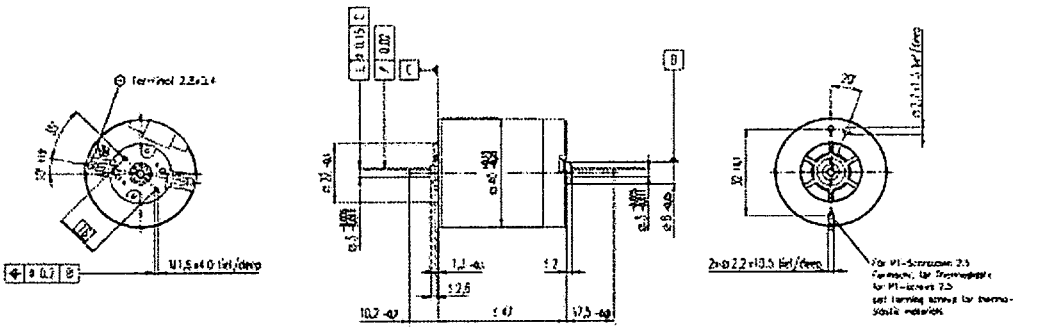

M 1:2

Stock program
Standard program
Special program (on request)

Order Number

2140. ... -50.236-050 (insert winding number)

Winding number		931	932	933	934	935	936	937	939
Motor Data									
1 Assigned power rating	W	6.0	6.0	6.0	6.0	6.0	6.0	6.0	6.0
2 Nominal voltage	Volt	6.0	9.0	9.0	12.0	15.0	18.0	24.0	36.0
3 No load speed	rpm	3540	4310	3490	3980	3900	3710	3960	4030
4 Stall torque	mNm	26.3	34.4	27.9	31.2	31.6	29.5	31.9	31.1
5 Speed / torque gradient	rpm / mNm	152	138	136	132	130	132	130	134
6 No load current	mA	56	47	35	30	24	18	15	10
7 Starting current	mA	1830	1870	1230	1130	808	669	578	378
8 Terminal resistance	Ohm	3.26	4.81	7.35	10.7	16.5	26.9	41.5	95.2
9 Max. permissible speed	rpm	11000	11000	11000	11000	11000	11000	11000	11000
10 Max. continuous current	mA	939	801	572	475	364	303	244	162
11 Max. continuous torque	mNm	12.1	12.7	13.0	13.2	13.4	13.4	13.6	13.3
12 Max. power output at nominal voltage	mW	2240	3660	2400	3030	3110	2770	3230	3200
13 Max. efficiency	%	81	86	65	67	68	68	69	70
14 Torque constant	mNm / A	14.4	18.4	22.7	27.8	34.8	44.1	55.2	82.3
15 Speed constant	rpm / V	664	519	420	344	276	216	173	116
16 Mechanical time constant	ms	36	33	33	32	31	31	30	30
17 Rotor inertia	gcm²	22.9	23.5	23.2	23.0	22.7	22.1	22.1	21.1
18 Terminal inductance	mH	0.34	0.56	0.85	1.27	1.99	3.21	5.02	11.20
19 Thermal resistance housing-ambient	K / W	10	10	10	10	10	10	10	10
20 Thermal resistance rotor-housing	K / W	8.8	8.6	8.8	8.8	8.8	8.8	9.8	8.8
21 Thermal time constant winding	s	43	44	44	43	43	42	42	40

Figure 50: Motor Specifications

B: Code to generate Position and velocity reference

```
clear all;

x = [0 0.5 1 1.5 2 2.5 3 3.25 3.5 4 5 6 6.5 6.75 7 7.5 8 8.5 9 9.5 10 10.25 10.5 10.75 11];
y = [0 0.5 1 1.5 2 2.5 3 3 3 3 3 3 3 3 3 2.5 2 1.5 1 0.5 0 0 0 0 0];

dt = 1e-3;
t = 0:dt:11;

theta = spline(x,y,t);
plot(t,theta);
title('Linear Drive Displacement vs. Time');
xlabel('Time (seconds)');
ylabel('Drive Displacement (m)');
grid on;

hold on;
plot(x,y,'ro');
thetadot = [0 dt*diff(theta)];
figure;
plot(t,thetadot,'g');
title('Linear Drive Velocity vs. Time');
xlabel('Time (seconds)');
ylabel('Drive Velocity (m/s)');
grid on;

theta=[t;theta];
thetadot=[t;thetadot];

save theta.mat theta
save thetadot.mat thetadot
```

C: Bode Plot of Low-pass Filter

$Fi = 1 / ((s/100) + 1)^2$

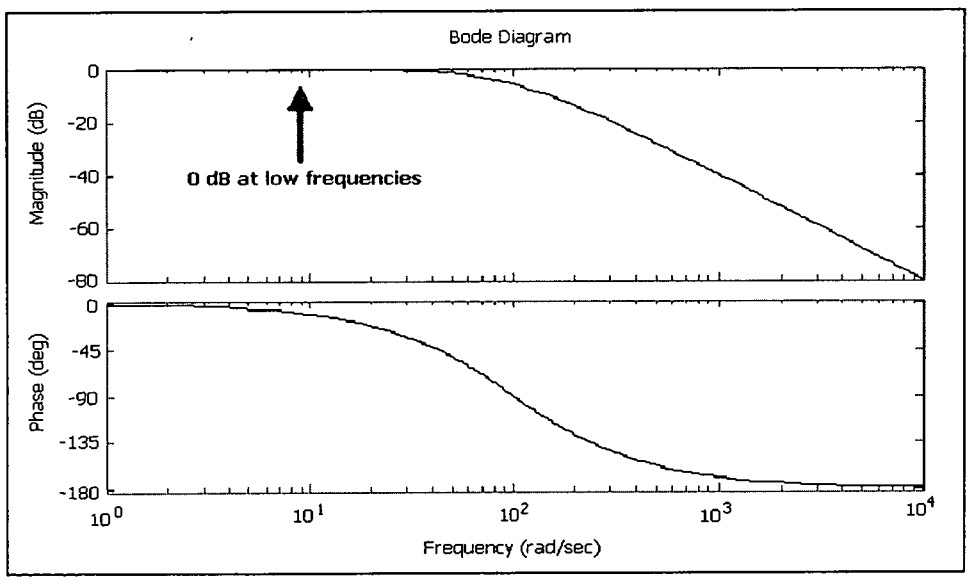

Figure 51: Bode Plot of Low-pass Filter

D: Collected data for System Modelling

Torque = 0.001

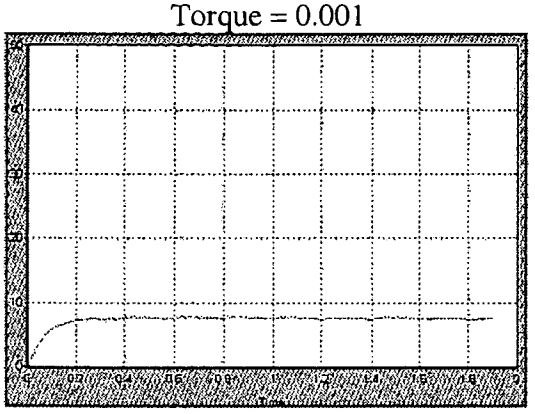

Torque = 0.002

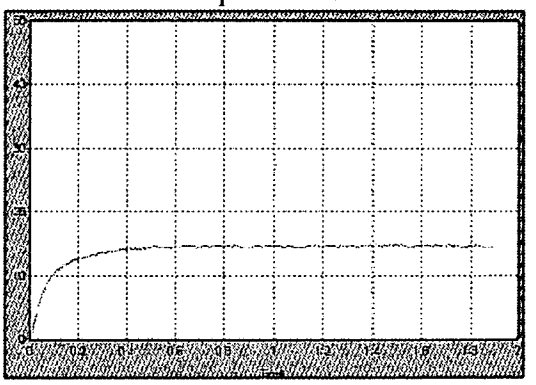

Torque = 0.003

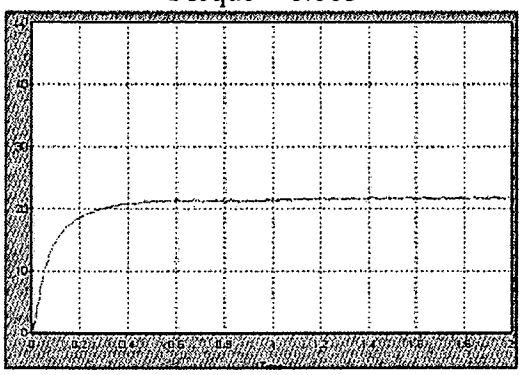

Torque = 0.004

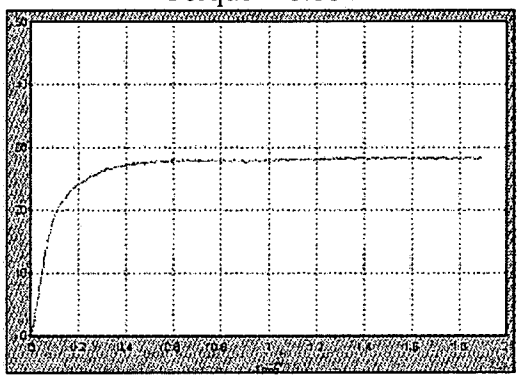

Torque = 0.005

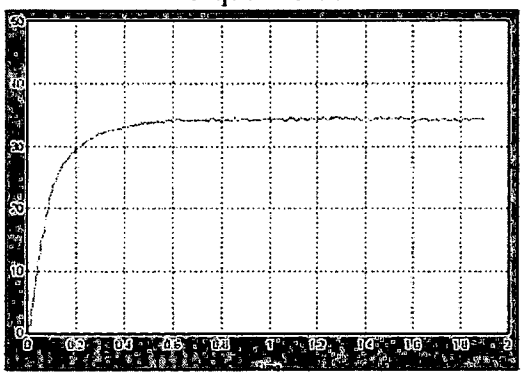

Torque = 0.006

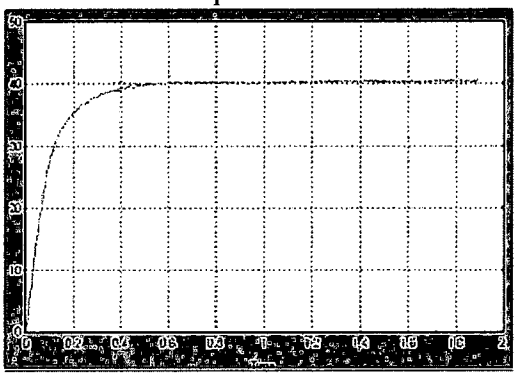

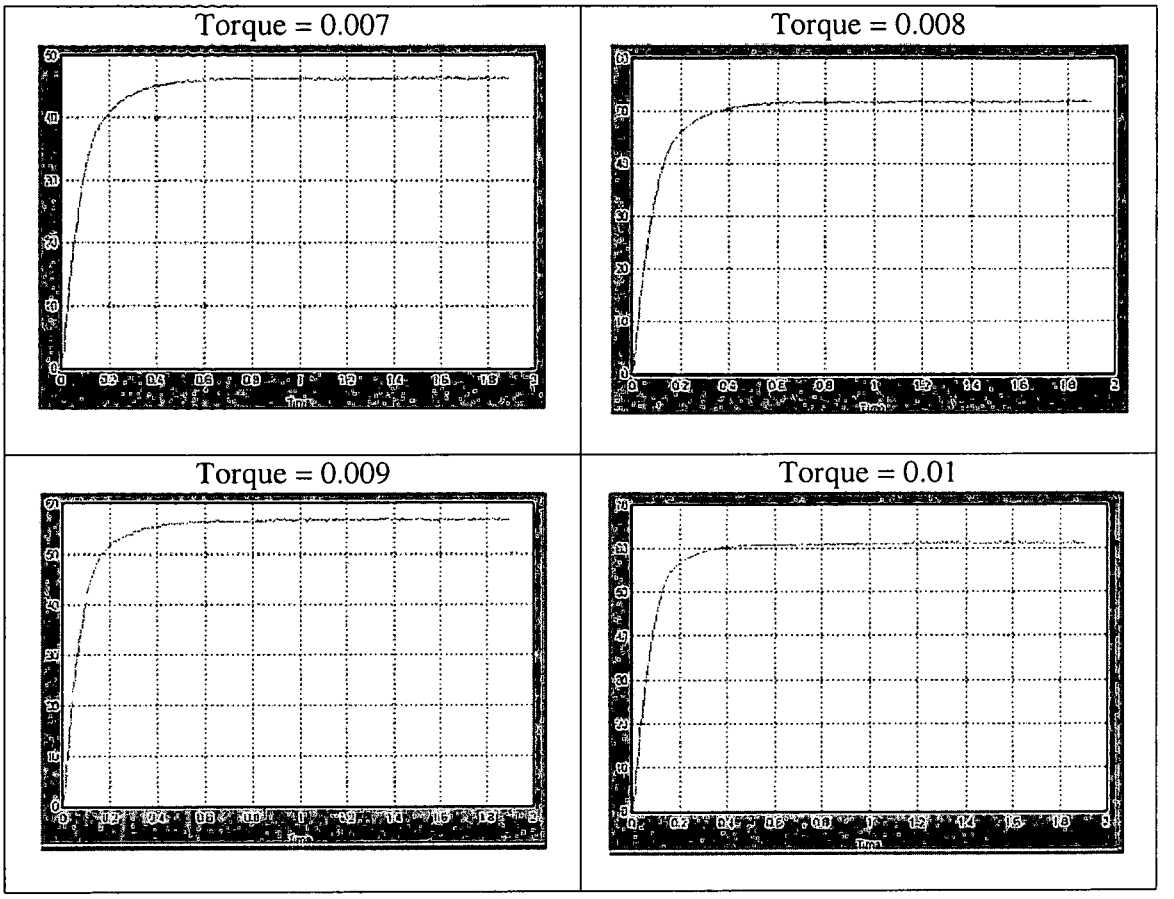

Figure 52: Torque Vs Velocity Responses

Torque	Theta	Time	acc	acc average	J=Mr2	Thetadot	d
0.001	0.018	0.01	360	219.0355556	4.56547E-06	7.586	0.000132
	0.046	0.02	230				
	0.089	0.03	197.7778				
	0.132	0.04	165				
	0.178	0.05	142.4				
0.002	0.021	0.01	420	292.7877778	6.83089E-06	14.483	0.000138
	0.061	0.02	305				
	0.121	0.03	268.8889				
	0.193	0.04	241.25				
	0.286	0.05	228.8				
0.003	0.018	0.01	360	269.0444444	1.11506E-05	21.379	0.00014
	0.05	0.02	250				
	0.118	0.03	262.2222				
	0.18	0.04	225				
	0.31	0.05	248				
0.004	0.018	0.01	360	333.2588889	1.20027E-05	27.586	0.000145
	0.071	0.02	355				
	0.146	0.03	324.4444				
	0.257	0.04	321.25				
	0.382	0.05	305.6				
0.005	0.025	0.01	500	414.7955556	1.20541E-05	34.483	0.000145
	0.086	0.02	430				
	0.179	0.03	397.7778				
	0.3	0.04	375				
	0.464	0.05	371.2				
0.006	0.021	0.01	420	455	1.31868E-05	40	0.00015
	0.093	0.02	465				
	0.207	0.03	460				
	0.38	0.04	475				
0.007	0.032	0.01	640	580.4513889	1.20596E-05	46.552	0.00015
	0.118	0.02	590				
	0.25	0.03	555.5556				
	0.429	0.04	536.25				
0.008	0.036	0.01	720	637.3263889	1.25524E-05	52.083	0.000154
	0.129	0.02	645				
	0.268	0.03	595.5556				
	0.471	0.04	588.75				
0.009	0.043	0.01	860	731.1111111	1.231E-05	57.5	0.000157
	0.16	0.02	800				
	0.24	0.03	533.3333				
0.01	0.046	0.01	920	820.5555556	1.21869E-05	60.476	0.000165
	0.175	0.02	875				
	0.3	0.03	666.6667				

Table 4: Calculated Values for System Model

D: Project Gantt Chart

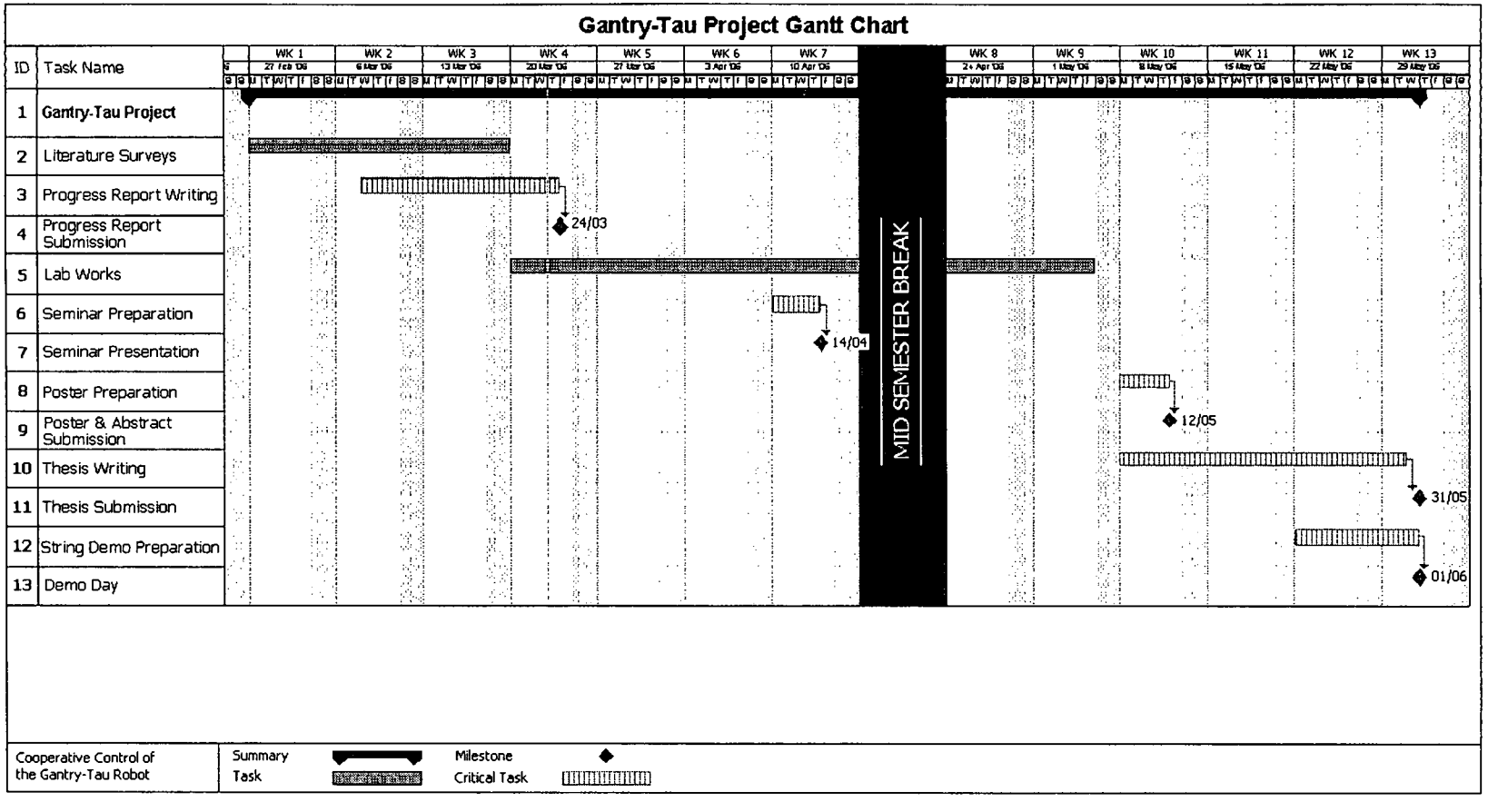

Figure 53: Project Gantt Chart

E: Tasks Allocation for Lab Works

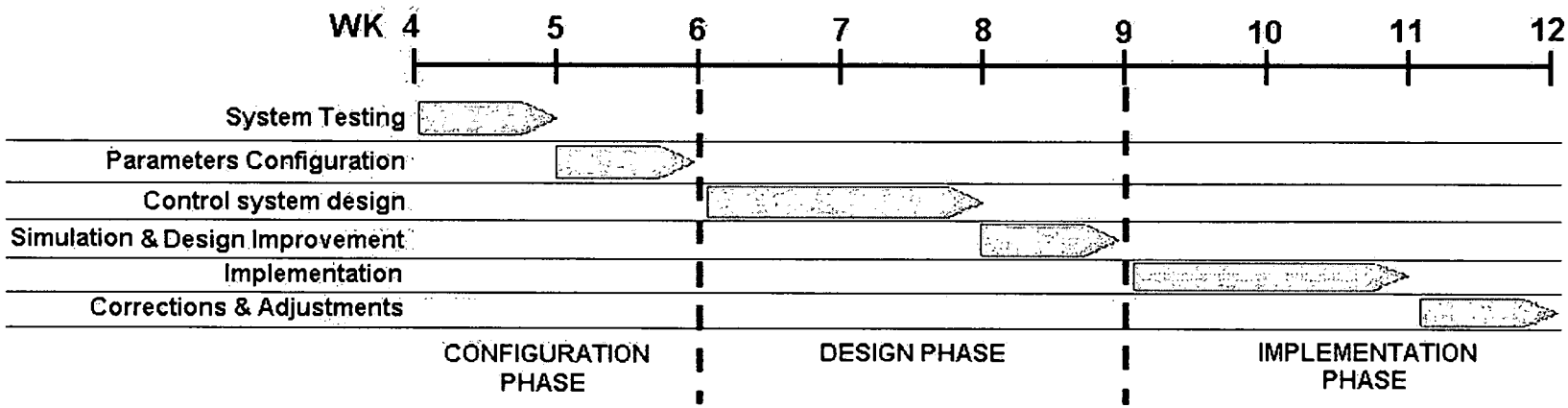

Figure 54: Lab Works Tasks Allocation